# CORTICAL REPRESENTATIONS OF AUDITORY AND TACTILE PERCEPTUAL DECISIONS

SETH M. LEVINE

A dissertation submitted to the Doctoral Program in Cognitive and Brain Sciences
in partial fulfillment of the requirements for the degree of
Doctor of Philosophy
(Ph.D.)

Under the supervision of
Prof. Dr. Jens V. Schwarzbach
Prof. Dr. Alfonso Carmazza

University of Trento, Center for Mind/Brain Sciences

October, 2015

*Dedicated to my parents,*
*the bravest people I know*

# TABLE OF CONTENTS

Table of figures ..... i

Table of tables ..... iii

1. Introduction ..... 1

Background ..... 1

Monkey neurophysiology ..... 2

Human neuroimaging ..... 4

Present work ..... 7

2. Parietal representations allow auditory and tactile perceptual decisions ..... 9

Abstract ..... 9

Introduction ..... 9

Materials and methods ..... 11

Participants and experimental sessions ..... 11

Auditory and tactile stimuli ..... 12

Stimulus presentation ..... 13

Experimental protocol ..... 13

Psychophysics ..... 14

Experimental design ..... 15

Neuroimaging data acquisition ..... 15

Behavioral data analysis ..... 16

Neuroimaging data analysis ..... 16

Results ..... 20

Behavioral results ..... 20

Neuroimaging results ..... 21

Conclusions ..... 27

3. Decoding supramodal information in human cortex ..... 31

Abstract ..... 31

Introduction ..... 32

Materials and Methods ..... 34

Participants and experimental sessions ..... 34

Experimental protocol and design ..... 35

Auditory and tactile stimuli ..... 35

Stimulus categories ..... 36

Stimulus presentation ..... 37

Neuroimaging data acquisition ..... 37

Behavioral data analysis ..... 38

Neuroimaging data analysis ..... 38

Results ..... 42

Behavioral results ..... 42

Neuroimaging results ..... 42

Discussion ..... 48

4. A new perspective for perceptual decision making ..... 53

Recapitulation ..... 53

Supramodality ..... 57

The bigger picture and future directions ..... 60

Conclusions ..... 64

References ..... 67

# TABLE OF FIGURES

Figure 2.1. Behavioral task and performance ..... 11

Figure 2.2. Univariate results ..... 22

Figure 2.3. Univariate conjunction results ..... 22

Figure 2.4. Multivariate results ..... 24

Figure 2.5. Multivariate conjunction results ..... 25

Figure 2.6. Patterns of category sensitivity. ..... 26

Figure 3.1. Trial protocol and stimulus categories ..... 34

Figure 3.2. Univariate results ..... 43

Figure 3.3. Multivariate results ..... 45

Figure 3.4. Cross-modality decoding results ..... 46

Figure 3.5. Functional connectivity results ..... 47

Figure 4.1. Cross-modal separability as a criterion for supramodality ..... 55

Figure 4.2. Theoretical function architectures ..... 59

Figure 4.3. Resource allocation as an amodal theoretical function ..... 59

# TABLE OF TABLES

Table 2.1. Regions obtained from univariate analyses ..... 23

Table 2.2. Regions obtained from multivariate analyses ..... 25

Table 3.1. Regions obtained from the univariate analysis ..... 43

Table 3.2. Regions obtained from the multivariate analysis of category II vs. category IV ..... 45

Table 3.3. Regions obtained from the multivariate analysis of category I vs. category III ..... 45

Table 3.4. Regions obtained from the cross-modality decoding analysis ..... 47

Table 3.5. Functional connectivity ..... 48

# 1. INTRODUCTION

The primary goal of this dissertation is to explore modality-general aspects of perceptual decision making in the human brain. Primarily, however, one must fully recognize a) the conceptual difference between *deciding* and *acting* and b) the importance of investigating perceptual decisions with the same "bottom-up" rigor as seen within the monkey neurophysiology literature. Upon the success of these two points, the field will be capable of designing paradigms to systematically remove confounds related to non-decision making processes; thus increasing our understanding of the neural representations of core decision making processes and improving our ability to study other, related theoretical cognitive mechanisms.

## BACKGROUND

Perceptual decision making (PDM) is commonly described as a scenario in which an observer must recognize who or what s/he is perceiving, while fog, rain, or some other kind of environmental noise is obscuring the setting, rendering the recognition process more difficult. This process has generally been theorized to consist of the accumulation of sensory evidence over time and has led to various attempts to link relevant model parameters to neural activity. For example, within a diffusion model framework, this accumulation is linked to increased neural firing, which eventually arrives at a firing threshold, representing the "decision boundary", the point in time at which the evidence is sufficient for a decision to be reached, regardless of the accuracy of the decision (Gold & Shadlen 2007, Heekeren et al. 2008). Alternatively, in an attractor network framework, the accumulation is explained through strong recurrent connections within a pool of selective excitatory neurons, whose activation by an external stimulus will drive the system from a spontaneous to a stable state (Deco et al. 2013,

Wang 2002, Wong & Wang 2006). Nevertheless, the results of such perceptual decisions are categorical outcomes, which has raised the argument that categorization is a fundamental, abstract computation of the decision making process (Freedman & Assad 2011).

## MONKEY NEUROPHYSIOLOGY

### VISUAL DECISION MAKING

Traditionally, the study of PDM at the neural level was carried out with monkeys trained to discern the direction of a patch of somewhat coherently moving dots on a screen, subsequently indicating their responses with an eye movement (saccade), while recordings were taking from neurons in either the middle temporal (MT) region of the brain (Britten et al. 1996, Newsome et al. 1989) or the lateral intraparietal (LIP) region (Shadlen & Newsome 1996, Shadlen & Newsome 2001). As the decision making process was theorized to include a "decision variable", which accumulated evidence over time (Shadlen et al. 1996), candidate regions to house such a variable would require neuronal spike rates that increased until a decision threshold has been reached.

It was discovered that the spike rate of LIP not only correlated with the percent coherence of the dot motion patch (i.e., signal quality) but also increased over time, until the monkey signaled his decision (Shadlen & Newsome 2001). Additionally, the neurons of the frontal eye fields (FEF) showed a similar spike rate accumulation, whose interruption with microstimulation also gave insight into a motor preparation stage of the process (Gold & Shadlen 2000). Consequently, the framework was laid out supporting the idea that regions such as LIP and FEF contained evidence integrators, which played key roles in perceptual decisions (Gold & Shadlen 2001, Gold & Shadlen 2007).

However, the paradigms often used tended to contain a major confound: namely that the monkey's decision regarding the stimulus was always linked to a predictable motor act: i.e., the way in which the response was signaled. As such, one could merely explain the spike rate accumulation as motor preparation (Schwarzbach and Caramazza, *in prep.*). This issue resulted in the need for a paradigm that dissociated perceptual decisions from motor acts (Freedman & Assad 2006). To this end, the researchers championed the delayed match-to-category paradigm, which essentially provides a subject with two back-to-back stimuli (separated by a delay), the first being a sample stimulus and the second being a test stimulus. The subject must then determine if the test matches the sample in terms of some feature (e.g., category membership), after which a motor act signaling the decision is executed, if the two stimuli do in fact match. By employing two stimuli per trial and requiring that any potential motor act depend on a *combination* of characteristics from the first and second stimuli, the first stimulus becomes essentially uncoupled from any systematic motor act, With this paradigm, Freedman and Assad (2006) led the way to a series of experiments, which demonstrated that categories of arbitrarily grouped visual stimuli could be represented by spike rates of LIP neurons (Fitzgerald et al. 2011, Swaminathan & Freedman 2012, Swaminathan et al. 2013). Shortly thereafter, Rishel et al. (2013) showed that such representations in LIP spike rates persisted through task-irrelevant saccades, despite LIP neurons *also* taking part in those saccades! Discussing their previous work and incorporating a study by Bennur and Gold (2011), Freedman and Assad put forth the idea that decisions may, thus, be represented by classifying stimuli into abstract categories: a process distinct from motor production and characterized by differences in LIP spike rates (2011). Although these PDM theories had been built on studies involving the visual system, non-visual domains had not been completely ignored.

## NON-VISUAL DECISION MAKING

In the meantime, a set of experiments was attempting to discover neural representations of tactile perceptual decisions by using a paradigm that tasked monkeys with discriminating and comparing the frequencies at which two back-to-back tactile stimuli fluttered along the fingertip (i.e., the monkeys indicated which stimulus' frequency was higher). In one such study, Salinas et al. (2000) probed neurons from primary somatosensory cortex and discovered that the resulting spike rates primarily represented simple stimulus encoding. However, shortly thereafter, when recording from secondary somatosensory cortex, the resulting spike rates appeared to represent a combination of the frequencies of the first and second stimuli (Romo et al. 2002). Unfortunately, these studies contained a similar confound in that the monkey's motor response was systematically correlated with one of the two stimuli, which possibly accounts for further studies demonstrating PDM processes within the medial and ventral premotor cortices (Hernandez et al. 2002, Romo et al. 2004).

With respect to the auditory domain, as mentioned by Heekeren et al. (2008), unfortunately no studies have robustly investigated auditory perceptual decisions in monkeys, with the exception of demonstrations that the primary auditory cortex of monkeys does not seem to play a role in auditory decisions beyond that of early stimulus encoding (Lemus et al. 2010, Lemus et al. 2009).

# HUMAN NEUROIMAGING

## VISUAL DECISION MAKING

Investigations of perceptual decision making within human cortex have produced a slew of neuroimaging studies, which have tried to link evidence accumulation, categorization, and other

decision making processes to regions such as dorsolateral prefrontal cortex (Heekeren et al. 2004, Heekeren et al. 2006, Philiastides et al. 2011), insular cortex (Grinband et al. 2006, Ho et al. 2009), and inferior and posterior parietal cortices (Hebart et al. 2012, Ploran et al. 2007). One primary issue within much of the human PDM literature, analogous to that of the monkey literature, is that motor confounds have not been robustly addressed. Often these functional magnetic resonance imaging (fMRI) studies have tasked participants with a simple discrimination of a visual stimulus (Heekeren et al. 2004, Heekeren et al. 2006, Ho et al. 2009) and a subsequent corresponding motor response to indicate his/her choice. This motor confound is potentially even more dangerous for an accurate interpretation of results given the poor temporal resolution of fMRI.

## NON-VISUAL DECISION MAKING

Moreover, although perceptual decision making studied in humans has delved further into the auditory and tactile domains than monkey studies, the paradigms used have often fallen into the same trap of insufficiently dissociating deciding from acting. As a result, similar regions of frontal cortex have also been, potentially erroneously, implicated in these auditory (Binder et al. 2004, Kaiser et al. 2007, Myers et al. 2009) and tactile studies (Pleger et al. 2006, Preuschhof et al. 2006).

Nevertheless, auditory PDM has been explored much further in humans than in monkeys, possibly attributable to the overwhelming use of audition for language. Thus, it seems reasonable to study auditory decisions through the lens of language: the exact route taken by many investigators who employed paradigms that required discrimination of linguistic syllables (Binder et al. 2004, Kaiser et al. 2007, Lee et al. 2012, Myers et al. 2009) or natural categories (De Lucia et al. 2012, Noppeney et al. 2010).

One immediate inconsistency arises in that the previously mentioned visual and tactile studies required participants to make decisions along some dimension of random-dot motion patches, faces/houses, or tactile frequency flutters: "lower-level" stimuli with relatively simple characteristics or stimuli with reliable activation patterns (e.g., face/house representations in the fusiform gyrus/parahippocampal cortex, respectively). In this way, researchers attempted to study aspects of decision making with less influence from "higher-level" cognitive processes. In contrast, by employing linguistic or natural categories as stimuli, the previously mentioned auditory studies may, in fact, be tapping into linguistic or semantic processes rather than only mechanisms of auditory decision making. Given that earlier studies have shown the recruitment of frontal regions during tasks that involve language or semantic processing (Lee et al. 2012, Roskies et al. 2001, Siok et al. 2003, Thompson-Schill et al. 1997), lower-level components of the auditory PDM process may be overlooked or undetectable when such linguistic or semantically-charged stimuli are present in a paradigm.

Importantly, recent studies have looked into auditory category representations (Leaver & Rauschecker 2010, Staeren et al. 2009) or made use of "lower-level" stimuli, such as frequency-modulated sweeps (Hsieh et al. 2012). However, such studies contain two pitfalls: the paradigms required no decision making from the participants regarding the stimuli, and the investigations bias themselves toward the temporal lobes. Although studies of this sort (including those containing linguistic stimuli) are interesting in their own regard and do contain their merits, exploring general mechanisms of decision making will require, firstly, paradigms optimized for decision making[1], an issue made more clear by McKee et al. (2014), who showed that certain brain regions only carried task-relevant information during decision

[1] Here I implicitly stress the difference between *deciding* and *acting*

making but not during passive viewing, and, secondly, whole-brain analyses, following the possibility that general decision making processes need not reside near sensory cortices.

## PRESENT WORK

The neuroimaging experiments presented in this dissertation are organized into three experiments within two chapters and encompass perceptual decisions based on audition and somatosensation, following the observation that these sensory systems are far less represented in the neuroimaging literature than studies based on vision. The experiments of chapter two attempt to challenge the idea that the frontal lobes are the main seat of category-specific information in perceptual decision making in a twofold manner: first, by putting emphasis on the need to disentangle deciding from acting—via a paradigm that dissociates stimulus categorization from predictable motor responses (Freedman & Assad 2006)—and, secondly, by utilizing relatively simple stimuli (i.e., auditory and tactile frequency sweeps) that are not "semantically charged" or otherwise linked to natural categories.

While the second chapter touches upon and makes claims about domain-general characteristics of abstract categorization in the human brain, the third chapter contains a follow-up experiment specifically designed to investigate such domain-generality. This second study sought to equate the auditory and tactile sensory modalities at an abstract level with the intention of uncovering which brain regions whose underlying information processing may be inherently supramodal. To this end, the dissertation ultimately changes direction and focuses on "supramodality". In doing so, both experiments are taken into consideration in an attempt to theorize that underlying processes within the framework for PDM may abstract away from both in the input channel (the sensory modality from which stimuli originate) and the output channel (the eventual overt motor act).

Our methodology-of-choice was functional magnetic resonance imaging (fMRI) coupled with multivariate pattern analysis (MVPA)(Haxby et al. 2001, Kriegeskorte et al. 2006, Oosterhof et al. 2011) in order to try to understand how spatially distributed patterns of observed data may represent potentially supramodal information that pertains to the categorization process.

# 2. PARIETAL REPRESENTATIONS ALLOW AUDITORY AND TACTILE PERCEPTUAL DECISIONS


## ABSTRACT

Perceptual decision making is the process that makes a rich environment manageable by compartmentalizing stimuli into various categories. Parietal cortex is involved in many tasks that require perceptual decisions. While much work in both the human and monkey domains has investigated processes related to visual decision making in the frontal and parietal lobes, relatively little research has explored auditory and tactile perceptual decisions. As such, we wanted to know whether these regions also play a role in auditory and tactile decision making. Using functional magnetic resonance imaging on humans and a paradigm specifically designed to avoid motor confounds and minimize linguistic processing, we found that one area in the right intraparietal sulcus, rather than any frontal regions, contained high-level abstract representations of auditory and tactile category-specific information. A further analysis revealed that encoding of information within this region is spatially distributed rather similarly between the auditory and tactile modalities, suggesting the presence of an underlying modality-general function. Whereas recent human neuroimaging studies have focused on the role of frontal areas in decision making and parietal areas in action selection, our findings advance the idea that parietal cortex represents information that abstracts away from both the input and output domains.


## INTRODUCTION

Parietal cortex seems to be involved in many different perceptual tasks (Hebart et al. 2012, Simanova et al. 2014, van Kemenade et al. 2014, Woolgar et al. 2011). So what is the role of the

parietal cortex in decision making? One stance posits that all decisions eventually lead to motor acts, and, therefore, the neural activity observed in frontoparietal areas represents motor intentions (Cisek & Kalaska 2005, Gold & Shadlen 2001, Shadlen & Newsome 2001), which do not distinguish between deciding and acting, and therefore is theoretically inseparable (Cisek & Kalaska 2010, Shadlen et al. 2008). However, this view has been criticized by studies that have expressly sought to decouple decisions from motor acts (Filimon et al. 2013, Freedman & Assad 2006).

Alternatively, one can posit that the role of parietal cortex in perception is to represent stimuli on different levels that abstract away from low-level properties, stimulus modalities (i.e., supramodal representations), and/or motor intentions (Eger et al. 2003, Freedman & Assad 2006, Rishel et al. 2013). This raises the question of whether parietal cortex contains different compartments for different sensory modalities, or whether it contains supramodal representations or even supramodal functions, such as categorization (Freedman & Assad 2011). We tested these ideas in the auditory and tactile domains with functional magnetic resonance imaging (fMRI) and multivariate pattern analysis (MVPA) (Haxby et al. 2001).

To investigate abstract auditory (aud) and tactile (tac) categorization in human cortex, we conducted two different fMRI experiments in which participants ($n_{aud}$ = 21, $n_{tac}$ = 19) performed a delayed match-to-category task (Figure 2.1B) that consisted of categorizing the direction (up or down) of frequency-modulated (FM) auditory or tactile sweeps of various magnitudes (Figure 2.1B). A given trial comprised a sample stimulus, a variable delay, and then a test stimulus. Participants were instructed to push a button when the sweep direction of the sample (S1) and test (S2) matched. This paradigm actively engages participants in decision making (McKee et al. 2014) and dissociates the overt response from stimulus categorization (Freedman & Assad 2006).

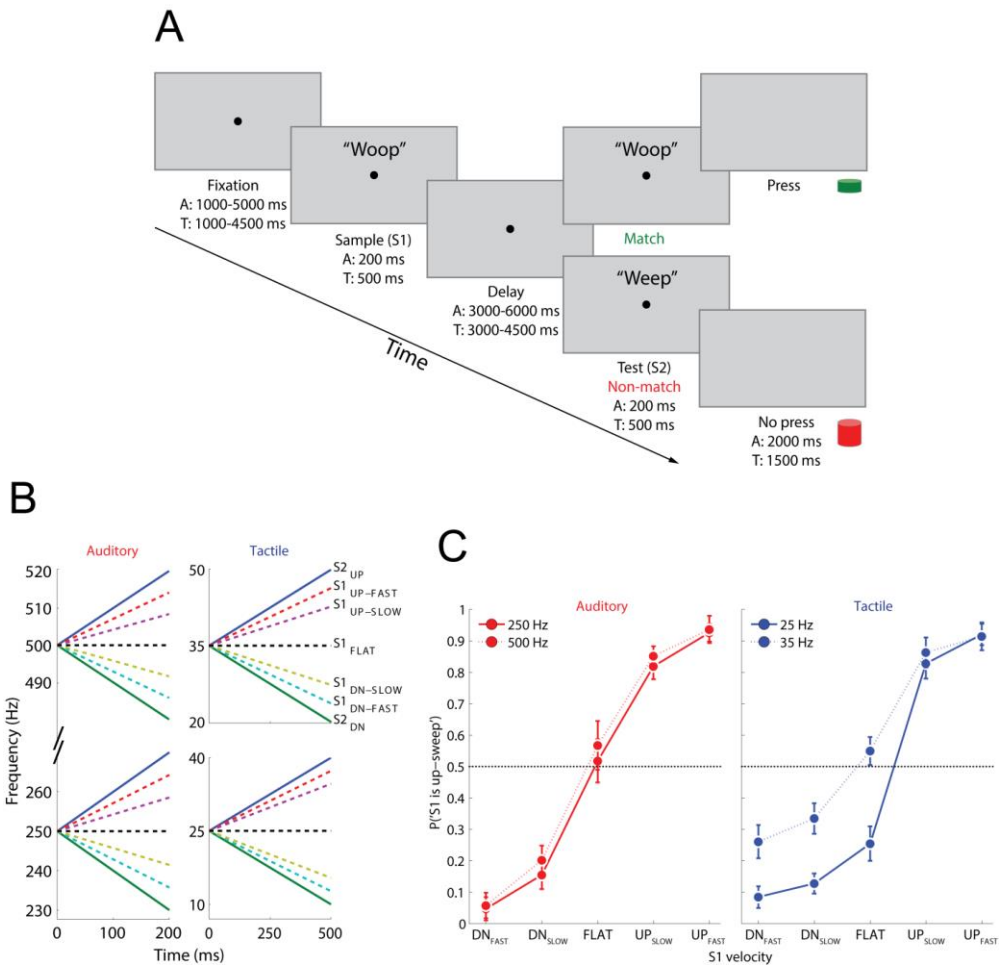


Figure 2.1. Behavioral task and performance

**(A)** Example trial of the auditory delayed match-to-category task. 'Weep' and 'woop' portray up- and down-sweeps. The fixation dot disappeared during the intertrial interval (1000–4000 ms). **(B)** FM-sweep stimuli in the experiment. For each experiment, stimulus frequencies began at their respective y-axis intercepts and swept upward (blue, red, and purple lines) or downward (green, cyan, and gold lines) for 200ms. S2 (solid lines) maintained constant sweep speeds, while those for S1 (dashed lines) were determined for each participant using an adaptive procedure[31]. Depicted S1's are average fast sweeps (red and cyan lines, A: ~70 Hz/s, T: ~12 Hz/s), average slow sweeps (purple and gold lines, A: ~40 Hz/s, T: ~9 Hz/s), and flat tones (black lines, 0 Hz/s). **(C)** Group-level probability that participants perceived S1 as an up-sweep for each of the stimulus velocities. Dashed lines denote chance-performance; error bars represent within-subjects 95% confidence intervals.

# MATERIALS AND METHODS

## PARTICIPANTS AND EXPERIMENTAL SESSIONS

Twenty-two (12 females and 10 males, 29.7±8.7 (μ±σ) years old) and 20 (11 females and 9 males, 29.3±7.8 years old) healthy subjects participated in the auditory and tactile experiments,

respectively, after providing written consent. All procedures followed safety guidelines for MRI research in the Laboratory for Functional Neuroimaging at the Center for Mind/Brain Studies (CIMeC) and were approved by the ethics committee of the University of Trento. Subjects engaged in a threshold acquisition session prior to the main experiment. One participant's auditory dataset was removed from analyses due to the participant having allegedly fallen asleep during experimentation, and one participant's tactile dataset was removed from analyses due to unusually poor behavioral results (Z(d') < -1.65). Six participants took part in both experiments.

## AUDITORY AND TACTILE STIMULI

The frequency sweeps were created using MATLAB (The Mathworks, Natick, MA, USA). Each sweep **y** was generated by the equation

$$\boldsymbol{y}=\sin(2\pi \boldsymbol{f}\cdot \boldsymbol{t})$$

where $\boldsymbol{f}$ is a vector of the sweep's frequencies at a given time point, $\boldsymbol{t}_{aud}$ is a 200 ms vector sampled at 44.1 kHz while $\boldsymbol{t}_{tac}$ is a 500 ms vector sampled at 1Khz, and $\boldsymbol{f}\cdot\boldsymbol{t}$ is the element-wise product of vectors $\boldsymbol{f}$ and $\boldsymbol{t}$. Each sweep's initial frequency at $\boldsymbol{t}_{aud}$ = 0 ms was either 250 Hz or 500 Hz (alternating between runs), while at $\boldsymbol{t}_{tac}$ = 0 ms they were either 25 Hz or 35 Hz (pseudorandomized across trials). The sweeps' final frequencies at $\boldsymbol{t}_{aud}$ = 200 ms and $\boldsymbol{t}_{tac}$ = 500 ms were determined by the condition of the trial (i.e., sweep direction: up/down and sweep speed: fast/slow/flat). All auditory stimuli had a 5 ms rise/fall amplitude envelope. Refer to Figure 1B for a visual depiction of the stimuli.

## STIMULUS PRESENTATION

Auditory, tactile, and visual stimulation were carried out using ASF (Schwarzbach 2011), built on the Psychophysics toolbox (Brainard 1997) for MATLAB. Visual stimuli (black fixation dots on a gray background) were projected behind participants in the MR scanner onto a semitransparent screen by means of an LCD projector (Epson EMP 9000) at a frame rate of 60 Hz and a resolution of 1280 x 1024 pixels and were viewed via a mirror positioned above the head coil. Auditory stimuli were presented binaurally through MR-compatible headphones (SereneSound, Resonance Technology, Northridge, CA, USA). Tactile stimuli were presented to the tip of the left index finger using a piezoelectric stimulator (Piezostimulator, QuaeroSys, Schotten, Germany), which contained a 2 × 4 matrix of pins (each 1 mm in diameter) that extended and retracted from a flat surface measuring 4 mm × 8 mm.

## EXPERIMENTAL PROTOCOL

The main experimental sessions were rapid event-related designs. The auditory experiment was organized into 6 runs (3 runs of stimuli at 250 Hz, 3 runs at 500 Hz) each containing 44 trials. A given trial (Figure 2.1A) contained a jittered, pre-stimulus fixation dot of 1000-5000 ms (geometrically distributed, p = 0.2), followed by a 200 ms sample sweep (S1), followed by a jittered delay of 3000-6000 ms (uniformly distributed, in steps of 750 ms), and then a 200 ms test sweep (S2), after which the participant was to immediately press a button with the right index finger if S2's sweep direction matched that of S1. Otherwise, no motor action was performed. In the case of S1's speed being 'flat', a response was considered correct when no button was pressed. There was a jittered, intertrial interval of 1000-4000 ms (uniformly distributed, in steps of 500 ms) during which the fixation dot disappeared.

Although similar in design, the timing of the tactile experimental differed slightly from that of the auditory experiment. Because we conducted the tactile experiment after the auditory experiment, we were able to improve the timing scheme for each trial, which was intended to decrease experimental time for the comfort of the participants.

Each run of the tactile experiment contained 56 trials and was similar to the auditory experiment, although the trial protocol made use of more efficient timing (Figure 2.1A). A given trial comprised a jittered, pre-stimulus fixation dot of 1000-4500 ms (geometrically distributed, $p = 0.2$), followed by a 500ms sample sweep (S1), followed by a jittered delay of 3000-4500 ms (uniformly distributed, in steps of 500 ms), and then a 500 ms test sweep (S2); the response logic was identical to that of the auditory experiment. The fixation dot disappeared during the intertrial interval, which also lasted 1000-4000 ms, but was uniformly distributed in steps of 750 ms. For technical reasons, two subjects performed the tactile task with a high-frequency condition of 40 Hz instead of 35 Hz.

## PSYCHOPHYSICS

The threshold acquisition session was composed of the same paradigm used in the main experiment but was a faster, non-jittered version using an adaptive procedure that converged on a participant's ~80% psychophysical threshold (García-Pérez 2000). Thresholds were acquired in the MR scanner in order to account for the background noise produced by the echoplanar imaging (EPI) sequence. The adaptive procedure consisted of 200 trials for the auditory experiment (100 trials of 250 Hz; 100 trials of 500 Hz) and 160 trials for the tactile experiment (80 trials of 25 Hz; 80 trials of 35 Hz), which was conducted second and adjusted for timing efficiency. Neuroimaging data acquired during the threshold acquisition session were not used.

## EXPERIMENTAL DESIGN

A given run of the auditory experiment was pseudorandomized and followed a 2 × 2 × 2 design: S1 direction × S1 speed × S2 direction, which broke down into Up/Down × Slow/Fast × Up/Down. S2 sweep speeds were held constant at 100 Hz/s (Figure 2.1B), while S1 slow sweeps corresponded to each subject's 80% threshold (42.3±10.6 Hz/s (μ±σ)), and S1 fast sweeps were half the distance between the slow sweep and the magnitude of S2. Each condition was repeated 5 times per run. Four trials (~10%) per run were control conditions, unknown to the participants, in which S1's sweep direction was flat (i.e., no frequency modulation), producing 2 flat trials when S2 swept upward and 2 flat trials when S2 swept downward.

Each run of the tactile experiment followed a 2 × 2 × 2 × 2 design: Base frequency × S1 direction × S1 speed × S2 direction, which broke down into Low/High × Up/Down × Slow/Fast × Up/Down. S2 sweep speeds were held constant at 15 Hz/s (Figure 2.1B), while S1 slow sweeps corresponded to each subject's 80% threshold (8.8±2.8 Hz/s (μ±σ)). Again, S1 fast sweeps were half the distance between the slow sweep and the magnitude of S2. Each condition was repeated 3 times per run, and 8 trials (~14%) per run were control conditions, in which S1 contained no frequency modulation.

## NEUROIMAGING DATA ACQUISITION

Data acquisition was carried out using a 4T Bruker MedSpec Biospin MR scanner and an 8-channel birdcage head coil. Functional images were acquired with a T2*-weighted gradient-recalled EPI sequence. At the beginning of each run we acquired a Point Spread Function (PSF) scan in order to reduce distortion in regions of high-field inhomogeneity (Robinson & Jovicich 2011, Zaitsev et al. 2004). We acquired 32 slices per volume in ascending interleaved order with a repetition time (TR) of 2250 ms (voxel resolution: 3-$mm^3$ in-plane, echo time (TE): 33

ms, flip angle (FA): 75°, gap-size: 0.45 mm). Of the 22 participants in the auditory experiment, 17 completed 6 runs of the experiment, 2 completed 5 runs, and 3 completed 4 runs (as a result of time constraints or fatigue/discomfort). Of the 19 participants in the tactile experiment, 1 completed 6 runs, 17 completed 5 runs, and 2 completed 4 runs.

For coregistration of the functional images to high-resolution anatomical images, we acquired a T1-weighted scan using a Magnetization-Prepared Rapid Gradient Echo sequence (MP-RAGE, 176 axial slices, field of view 256mm x 224mm, 1-$mm^3$ isotropic voxels, Generalized Autocalibrating Partially Parallel Acquisition (GRAPPA) with acceleration factor = 2, TR = 2700 ms, TE = 4.180 ms, TI = 1020 ms, FA = 7°) for each participant.

## BEHAVIORAL DATA ANALYSIS

A two-way analysis of variance was computed on the participants' accuracies using ezANOVA (Rorden, mccauslandcenter.sc.edu/mricro/ezanova) with factors base frequency (auditory: 250 Hz, 500 Hz; tactile: 25 Hz, 35 Hz) and sweep velocity (Down-Fast, Down-Slow, Flat, Up-Slow, Up-Fast) (Figure 2.1C). Only the trials in which participants correctly categorized the stimuli were included in the neuroimaging analyses.

## NEUROIMAGING DATA ANALYSIS

Analysis of the acquired neuroimaging data was carried out with Brainvoyager QX 2.8 (Goebel et al. 2006) and the Neuroelf software package (Weber, neuroelf.net).

### PREPROCESSING

The acquired PSF data were used to apply distortion correction to the EPI images (Zaitsev et al. 2004). Next, the first three volumes of each functional scan were discarded to account for signal

saturation. Preprocessing of the functional data included, in the following order, slice time correction (cubic spline interpolation), motion correction with respect to the first (remaining) volume in the first run (estimation with trilinear, resampling with sinc interpolation), and temporal highpass filtering (cutoff: 3 cycles within the run). For each participant, functional data were then co-registered to high-resolution, de-skulled anatomical scans in native space; subsequently, echo-planar and anatomical volumes were transformed into standardized space (Talairach & Tournoux 1988).

## CORTEX BASED ALIGNMENT

Due to high variability in cortical anatomy between subjects, we performed a cortex-based alignment in an effort to increase the accuracy of the localization of effects at the group-level (Fischl et al. 1999). The cortical surface of each participant was segmented from the rest of the brain, and the resulting mesh surface was morphed into a sphere, after which the gyral/sulcal folding pattern was aligned to a group-average template sphere. This sphere-to-sphere alignment was then applied to each participant's functional data, such that further group-level statistics could be carried out on a standard 2D cortical surface constructed from participants in both experiments.

## UNIVARIATE ANALYSIS

Data were analyzed with a random-effects (RFX) general linear model (GLM). Regressors of interest, which were all combinations of features for S1 (Up/Down × Fast/Slow/Flat), all combinations of features for S2 (Up/Down × Match/Non-Match), the onset of the fixation dot, and the button press (whose onset was calculated from the reaction time), were modeled with a dual-gamma hemodynamic response function (HRF; onset = 0, time to peak = 5 s, dispersion = 1, undershoot ratio = 6, undershoot peak = 15 s, undershoot dispersion = 1). Motion correction

parameters for 6 directions (3 translational, 3 rotational) were modeled as regressors of non-interest.

## MULTIVARIATE PATTERN ANALYSIS

Conditions of interest (i.e., up-sweeps and down-sweeps) for a surface-based searchlight analysis (Kriegeskorte et al. 2006, Oosterhof et al. 2011, Oosterhof and Connolly, cosmomvpa.org) were selected, and single-trial GLMs were computed in volume space to produce maps of the resulting beta-weights' t-scores using the same parameters as in the previous GLM computation for the univariate analysis. Within each direction-of-interest (i.e., up or down sweep), these t-score patterns were then collapsed across sweep speed (fast/slow/flat), base frequency (low/high), and sample/test stimuli. These volume maps were sampled using the surfing toolbox (Oosterhof et al. 2011) in order to morph the functional data into surface maps, which were then passed to a linear support vector machine (SVM) implemented with LIBSVM (Chang & Lin 2011). The SVM (c = 1) attempted to classify the two conditions based on the pattern of t-scores across the vertices of the searchlight (r = 8 mm). Training/testing of the SVM followed a leave-one-run-out cross-validation procedure, and classification accuracy was computed for each permutation of the cross-validation. The resulting classification accuracy for a given vertex was the mean of the all the permutations' accuracies. This process was repeated at each vertex of the map. Accuracies were then converted to d'-values, and an 8-nearest neighbor smoothing kernel (~3.5 mm FWHM) was applied to individual subject d' maps before running group-level t-tests.

## CLUSTER-BASED THRESHOLDS

Given the importance of the cluster over the single voxel in neuroimaging data analysis (Penny & Friston 2003), for all tests we employed a cluster-based threshold (Friston et al. 1994) to

correct for multiple comparisons. As suggested by Woo et al. (2014), we employed an initial two-tailed threshold at $p < 0.001$ (This threshold proved too conservative for the multivariate analyses, which consequently made use of a slightly relaxed initial threshold of $p < 0.005$) and then ran a bootstrapping algorithm in which, for each subject's statistical parameter map, the sign of the d'-values was flipped with a probability of 0.5, the t-test across subjects was recomputed, and the conjunction across modalities was performed. This process was repeated 104 times for each hemisphere. On each iteration, the number of contiguous vertices of the largest cluster present in the map was computed to correct for the family-wise error rate (FWER) (Hayasaka & Nichols 2003), resulting in a null distribution of 104 cluster areas (N.B.: the smallest observable p-value for a cluster area is 0.0001).

## LOGICAL CONJUNCTION

In order to rule out brain areas that were involved in modality-specific processing, we computed the conjunction (Nichols et al. 2005) of auditory and tactile group-level maps by taking the smaller absolute value of the two t-scores at each vertex (which already independently surpassed a given threshold) and using the smaller of the two degrees of freedom for subsequent statistical analyses.

## PATTERN SIMILARITY ANALYSIS

To understand if there was any similarity between the two modalities within the right IPS region, we correlated patterns of category sensitivity distributed across the vertices of the region. Within a given modality, all participants' vectors of 51 unsmoothed d'-values pertaining to the right IPS patch were demeaned (participant-wise) and then pairwise correlations were computed vertex-wise, resulting in a 51 × 51 matrix of Pearon's r values (symmetric over the main diagonal; Figure 2.6A). The lower triangle (ignoring the main diagonal) was then extracted

from each modality's correlation matrix (Figure 2.6B), and we computed another Pearson's correlation of these two lower triangles (Figure 2.6C).

### MODALITY CORRELATION ANALYSIS

In order to see if there was a general relationship between the decoding of the auditory and tactile modalities within the region of the right IPS revealed by the conjunction analysis, we extracted the unsmoothed group-level mean d'-values at each of the region's 51 vertices for both modalities and calculated Pearson's r between them.

## RESULTS

### BEHAVIORAL RESULTS

Participants successfully discriminated up-sweeps from down-sweeps (Figure 2.1C). For the auditory results, a two-way analysis of variance confirmed that performance varied as a function of sweep velocity ($F_{(4, 80)} = 339$, $p < 10^{-6}$) but not of base frequency ($F_{(1, 20)} = 3.17$, $p < 0.09$). However, regarding the tactile results, the correct categorization of higher-frequency down-sweeps was partially diminished, and the ANOVA revealed main effects of both sweep velocity ($F_{(4, 72)} = 349$, $p < 10^{-6}$) and base frequency ($F_{(1, 18)} = 42.7$, $p < 4x10^{-6}$) and also an interaction between them ($F_{(4, 72)} = 16$, $p < 10^{-6}$).

## NEUROIMAGING RESULTS

### TASK ACTIVATES FEW REGIONS; NO UNIVARIATE BOLD DIFFERENCE FOR SWEEP DIRECTION

To discover cortical regions generally involved in stimulus categorization, we computed the univariate conjunction of all S1 and S2 predictors collapsed [S1 ∩ S2] (Nichols et al. 2005) on cortex-based aligned (Fischl et al. 1999) surfaces individually for the auditory and tactile modalities (Figure 2.2). We then computed the conjunction of these maps across modalities and applied a cluster-based threshold, revealing several areas (Figure 2.3, Table 2.1), whose BOLD amplitude changes and cluster areas survived their respective thresholds ($t_{(18)} = 3.922$, $p_{unc.} < 0.001$; $p_{cluster} < 0.01$, family-wise error rate corrected (FWER)). Although the univariate contrast [S1 Up > S1 Down] did yield clusters containing differences in BOLD amplitude for both modalities independently, these effects disappeared after the conjunction.

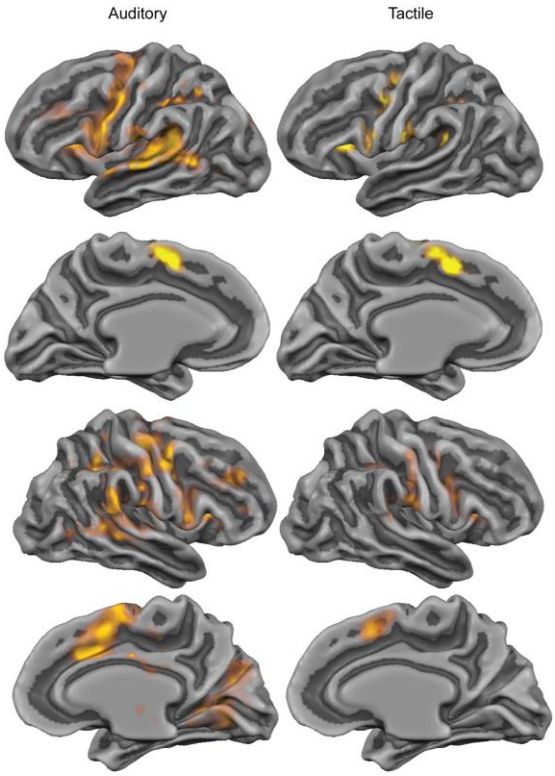


Figure 2.2. Univariate results

Uncorrected (from $p < 0.05$) group-level activation map revealed by the conjunction [S1 ∩ S2] visualized on a partially-inflated, cortex-based aligned, group-average brain. Transparency scales with the magnitude of the t-score.

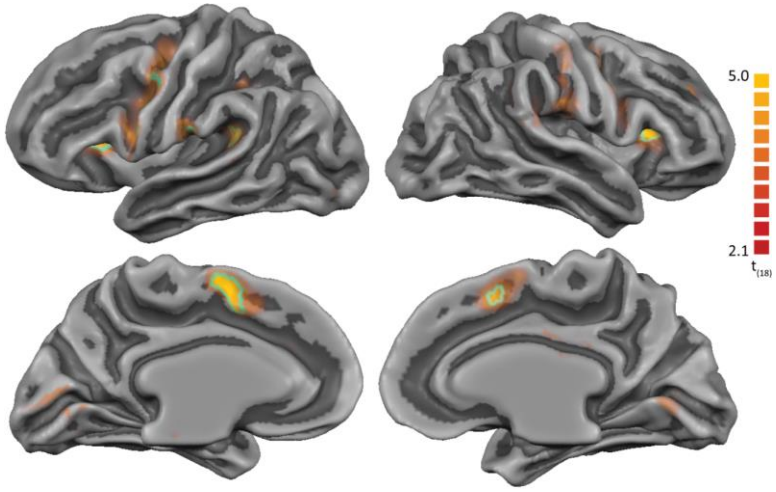


Figure 2.3. Univariate conjunction results

Uncorrected (from $p < 0.05$) group-level map revealed by the conjunction of each modality's univariate conjunction [S1 ∩ S2]. The light blue outlines depict regions that survived the cluster-based threshold ($p_{cluster} < 0.01$, FWER). Transparency scales with the magnitude of the t-score.

| Region | Hemisphere | Talairach coordinates (x, y, z) | # of vertices | $p_{cluster}$ | t-score | $p_{activation}$ |
|---|---|---|---|---|---|---|
| PT | L | (-49, -42, 20) | 112 | $10^{-4}$ | 4.78 | $1.5\times10^{-4}$ |
| MFG | L | (-7, 3, 57) | 91 | $10^{-4}$ | 5.37 | $4.2\times10^{-5}$ |
| aIns | L | (-26, 20, 12) | 59 | $10^{-4}$ | 5.05 | $8.3\times10^{-5}$ |
| PreCG | L | (-42, -6, 44) | 28 | $10^{-4}$ | 4.21 | $5.3\times10^{-4}$ |
| PrCv | L | (-53, 1, 23) | 24 | $10^{-4}$ | 4.29 | $4.4\times10^{-4}$ |
| aIPL | L | (-54, -22, 24) | 18 | $10^{-4}$ | 4.45 | $3.1\times10^{-4}$ |
| aIns | R | (29, 21, 15) | 61 | $10^{-4}$ | 5.08 | $7.9\times10^{-5}$ |
| MFG | R | (8, 8, 48) | 26 | $10^{-4}$ | 4.54 | $2.6\times10^{-4}$ |

Table 2.1. Regions obtained from univariate analyses

Descriptive statistics, after the conjunction between modalities, of the six left-hemisphere regions (medial frontal gyrus (MFG), planum temporale (PT), anterior insula (aIns), precentral gyrus (PreCG), ventral precentral sulcus (PrCv), anterior intraparietal lobule (aIPL)) and two right-hemisphere regions (medial frontal gyrus (MFG), anterior insula (aIns)) revealed by the univariate contrast [S1 ∩ S2], and the one right-hemisphere region (intraparietal sulcus (IPS)) revealed by multivariate SVM-decoding of up-sweeps versus down-sweeps. Multiple comparisons corrections were computed with a cluster-based threshold. Coordinates refer to the location of the peak t-score within a cluster.

## LOCAL PATTERNS OF ACTIVITY IN IPS REPRESENT SWEEP DIRECTION

We employed MVPA (Haxby et al. 2001) to uncover category representations distributed across multiple vertices (Oosterhof et al. 2011). Within each modality, a linear support-vector machine (SVM; Chang and Lin, 2011), implemented via surface-based searchlight (Kriegeskorte et al. 2006, Oosterhof et al. 2011), decoded up- from down-sweeps (collapsed across sweep speed, base frequency, and S1/S2) from a distributed network for both the auditory and tactile modalities (Figure 2.4). However, their conjunction revealed that only the intraparietal sulcus (IPS) of the right hemisphere (Figure 2.5, Table 2.2) contained category-specific information irrespective of sensory modalities ($t_{(18)} = 3.197$, $p_{unc.} < 0.005$; $p_{cluster} < 0.01$, FWER).

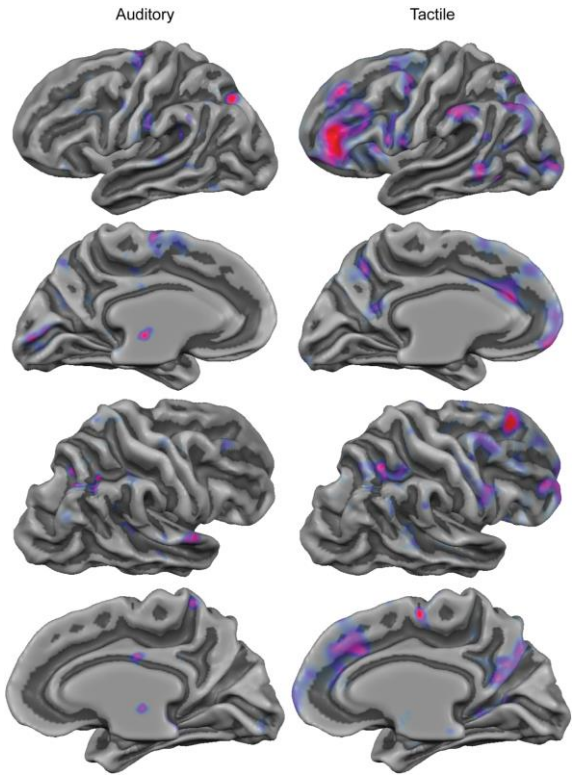


Figure 2.4. Multivariate results

Uncorrected (from $p < 0.05$) group-level t-scores of SVM classification of up-sweeps vs. down-sweeps. Same conventions as in Figure 2.2.

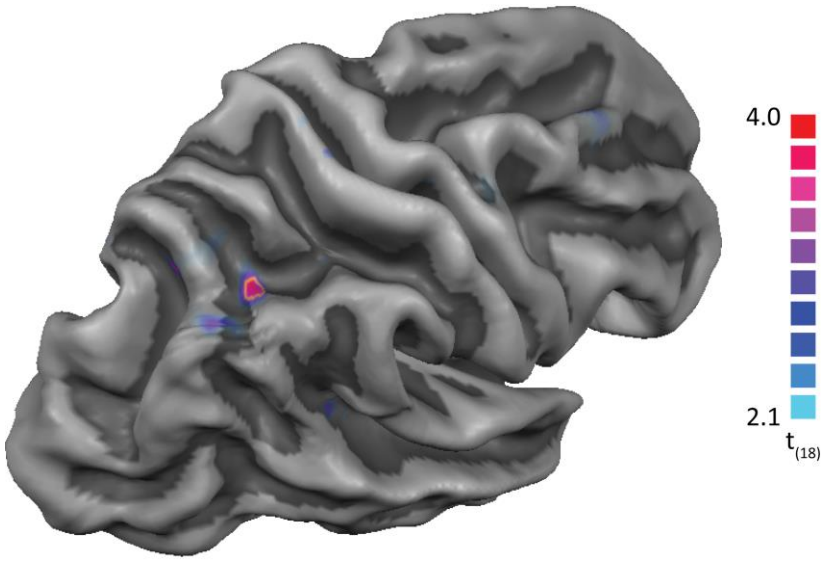


Figure 2.5. Multivariate conjunction results

Uncorrected (from $p < 0.05$) group-level t-scores of SVM classification of up-sweeps vs. down-sweeps, after the conjunction across modalities. The yellow outline depicts the only cluster that survived the cluster-based threshold ($p_{cluster} < 0.01$, FWER). Note the lack of overlap between the surviving clusters revealed by the multivariate and univariate (see Figure 2.3) analyses.

| Region | Talairach coords. (x, y, z) | # of vertices | $p_{cluster}$ | Decoding range: d' (%) | t-score | $p_{decoding}$ |
|---|---|---|---|---|---|---|
| IPS | (31, -53, 38) | 51 | $3.9\times10^{-4}$ | A: [0.05, 0.15] ([51.04, 52.98]) | 6.01 | $3.5\times10^{-6}$ |
| | | | | T: [0.06, 0.14] ([51.28, 52.86]) | 4.30 | $2.1\times10^{-4}$ |

Table 2.2. Regions obtained from multivariate analyses

Descriptive statistics, after the conjunction between modalities, of the one right-hemisphere region (intraparietal sulcus (IPS)) revealed by multivariate SVM-decoding of up-sweeps versus down-sweeps. Multiple comparisons corrections were computed with a cluster-based threshold. Coordinates refer to the location of the peak t-score within a cluster. 'A' and 'T' under the 'Decoding range' column refer to auditory and tactile, respectively.Patterns of category sensitivity within IPS are similar across modalities.

## PATTERNS OF CATEGORY SENSITIVITY WITHIN IPS ARE SIMILAR ACROSS MODALITIES

A region-of-interest analysis sought out any patterns of information present within the sensitivity maps of the IPS. The degree to which multivariate decoding correlated across different vertices of the IPS exposed distributed patterns of information for both modalities (Figure 2.6A). Most interestingly, however, these patterns distributed across rather similar vertices for both modalities (Pearson's $r = 0.55$, $p = 9.8 \times 10^{-103}$; Figure 2.6C).

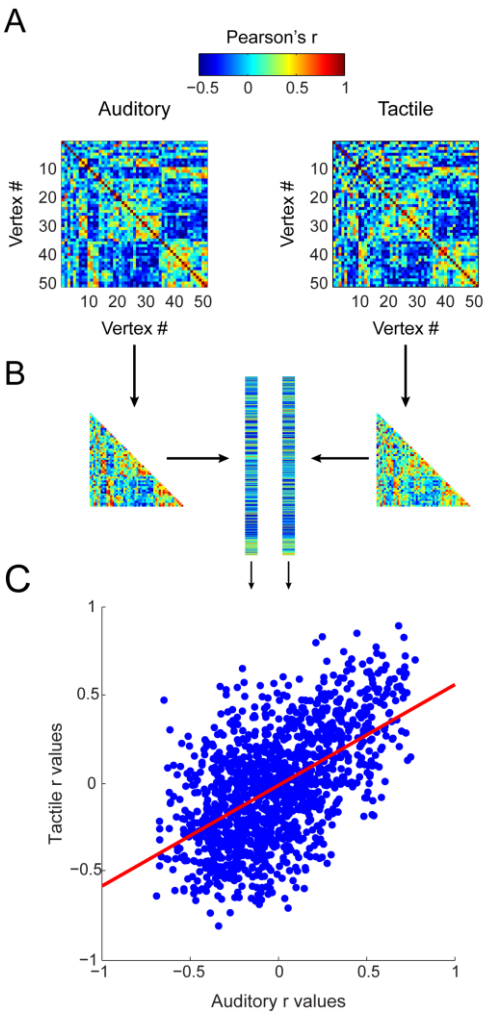


Figure 2.6. Patterns of category sensitivity.

**(A)** Correlating patterns of SVM classification sensitivities (d') within the IPS reveals a striking similarity between modalities in how the category information is decoded across the region. To quantify this similarity, **(B)** the lower left triangles were extracted from each matrix (ignoring the main diagonal) and **(C)** a linear correlation was computed on these vectors, revealing a rather high degree of agreement between the modalities (Pearson's r = 0.55) in how information was decoded within the region. The red line represents a least-squares best fit.

## IPS SHOWS NO PREFERENCE FOR MODALITY

A further region-of-interest analysis on the IPS, which attempted to uncover any modality bias within the region, showed no correlation (Pearson's r = -0.23, p = 0.11) between group-level mean auditory and group-level mean tactile d'-values of each vertex.

## CONCLUSIONS

A whole-brain multivariate searchlight exposed information encoded in patterns of activity and identified a single area in the right IPS that categorized FM-sweep direction. Given that the up vs. down categories that were fed into the SVM (and that participants learned) contained stimuli characterized by different base frequencies (Aud: 250 Hz or 500 Hz, Tac: 25 Hz or 35 Hz) and different sweep magnitudes (i.e., slow, fast, superfast sweep speeds), the categorical information learned by the SVM is unlikely to be linked to such physical stimulus properties. Furthermore, the conjunction between two independent experiments (i.e., one tactile, one auditory) removed regions that were inherently modality-specific from the analysis and consequently revealed a common area for representing high-level perceptual information. If these two sensory modalities were processed by two distinct perceptual decision making mechanisms in different regions, then we would not expect to find commonalities.

However, the SVM did not strongly decode up- from down-sweeps in regions revealed by the univariate conjunction [S1 ∩ S2] (Figure 2.4), despite these regions' activity likely reflecting task-relevant processing (Woolgar et al. 2011, Fedorenko et al. 2013). Not relying on univariate changes of BOLD differentiates our approach from earlier work on auditory (Binder et al. 2004, Noppeney et al. 2010, Tamber-Rosenau et al. 2013) and tactile (Pleger et al. 2006, Preuschhof et al. 2006, van Kemenade et al. 2014) processing of perceptual categories.

Previous reports on the involvement of frontal cortex in decision making (Binder et al. 2004, Pleger et al. 2006, Preuschhof et al. 2006, Philiastides et al. 2011) did not disentangle predictably associated motor acts from the decision process. By deconfounding motor acts from perceptual decisions, our findings suggest that, independent of coding actions and motor intentions (Shadlen et al. 2008), parietal cortex is involved in representing high-level abstract

information (Freedman and Assad, 2006, 2011). Collapsing the datasets across all dimensions except sweep direction ensured that physical stimulus properties within categories were different (reducing the likelihood that these properties influenced the SVM), while those between categories were similar. As a result, sweep direction was the predominant between-category difference yielding successful SVM training.

Given that previous work regarding the IPS has investigated supramodal numerosity (Eger et al. 2003), spatial processing (Yantis et al. 2002, Lehnert and Zimmer, 2008), category switching (Serences et al. 2004), and attention-based rehearsal in spatial working memory (Postle et al. 2004), our results allow us to set up a general theory that the IPS represents abstract information, independent of sensory modalities. However, because our findings are restricted to the right IPS, one possible explanation adheres to the idea of temporal information. Previous discussions by Battelli et al. (2007) have proposed that the right inferior parietal lobule is involved in temporal attention. While our results reveal categorical information, rather than mere task-related activation, one could argue that frequency sweeps (in either the auditory or tactile domain) inherently contain temporal features that exist in their cortical representations. Consequently, it is conceivable that the function of the right IPS is to represent temporal categories. Although converging evidence from physiological (Fitzgerald et al. 2011) and neuroimaging work (Heekeren et al. 2004, Hebart et al. 2012) has demonstrated the parietal lobe to be involved in visual categorization, a crucial test of our theory would consist of finding that the right IPS also encodes non-temporal visual categories. Testing beyond modality-general aspects of categorization (e.g., category flexibility) in the IPS will require future work to investigate a larger number of different arbitrary categories with alterable category boundaries.

Moreover, while the conjunction analysis indicates that the right IPS contains at least multimodal representations that are independent of motor acts, we ran two further correlation analyses to explore information within this region-of-interest. The first analysis revealed that patterns of category-sensitive information were distributed across rather similar vertices for both modalities (Figure 2.6), which speaks to a supramodal (rather than only a multimodal) interpretation of the role of the IPS. Furthermore, the second analysis revealed no correlation between mean auditory and mean tactile d'-values of each vertex, suggesting no particular compartmentalization of modalities within this region. One could further scrutinize the idea of supramodality by testing for cortical representations of inherently supramodal categories within this region, an analysis that is not possible with the current between-subjects design.

Taken together, our results reveal high-level abstract information encoded in the right IPS from two different sensory modalities. This finding, supported by previous work in the visual domain from monkey neurophysiology (Freedman and Assad, 2006, Fitzgerald et al. 2011) and human neuroimaging (Ploran et al. 2007, Hebart et al. 2012), suggests that, irrespective of motor affordances, the role of parietal cortex in decision making goes beyond that of general involvement (Ploran et al. 2007, O'Connell et al. 2012, Tamber-Rosenau et al. 2013) and instead leads to the working hypothesis that the right IPS is a categorizer that abstracts away from both the input and output domains.

# 3. DECODING SUPRAMODAL INFORMATION IN HUMAN CORTEX


## ABSTRACT

Perceptual decision making is the cognitive process whereby the brain parcels stimuli into abstract categories. Most prior work has probed the underlying processes in a unimodal fashion, leaving the question of supramodal categorization open to speculation. To investigate supramodal categorization, one must ensure that supramodal information exists at some level of the functional architecture by abstractly equating different sensory modalities—independent of temporal or spatial information. We employed a delayed match-to-category paradigm requiring participants to categorize auditory and tactile frequency-modulated (FM) sweeps according to learned, supramodal categories. While participants performed this task, we measured their blood-oxygenation-level dependent signal using functional MRI. To detect cortical representations of supramodal information, we used whole-brain multivariate pattern analysis implemented via linear discriminant analysis (LDA) classification. With three different analyses we showed that a) learned categories were best decoded within the right anterior parietal lobe and the medial frontal gyrus, b) supramodal representations of "up- vs. down-sweeps" were localized to the left parietal-temporal-occipital junction, and, most consequentially, c) cross-modality decoding of category membership was strongest in the left posterior insula and precuneus. Given our choice of paradigm, such results appear to demonstrate that the information representations in the posterior insula and precuneus are independent of motor and language processing and instead reflect supramodal or modality-free mechanisms that underlie the categorization process.

# INTRODUCTION

Interacting with the environment stimulates all of our senses. Although this may seem overwhelming, cognition makes life manageable by breaking down sensory stimulation into simple categories. The functions that the brain utilizes to integrate such sensory information over time (Gold & Shadlen 2007, Heekeren et al. 2008) and parcel it into abstract categories (Freedman & Assad 2011) are part of the process known as perceptual decision making. However, the extent to which this process abstracts away from the sensory domain remains unknown.

Previous neuroimaging work in humans has used visual (Grinband et al. 2006, Hebart et al. 2012, Heekeren et al. 2004, Ho et al. 2009, Ploran et al. 2007), auditory (Binder et al. 2004, Kaiser et al. 2007, Lee et al. 2012, Myers et al. 2009), and tactile (Pleger et al. 2006, Preuschhof et al. 2006, van Kemenade et al. 2014) stimulation to probe the cortical mechanisms that underlie the process of categorization. Furthermore, some investigations have even sought to understand perceptual decisions irrespective of sensory modalities (Ivanoff et al. 2009, Noppeney et al. 2010, O'Connell et al. 2012, Simanova et al. 2014, Tamber-Rosenau et al. 2013, Levine & Schwarzbach *under review*). However, no study so far has tried to explicitly equate sensory modalities within the perceptual task, effectively ensuring modality-general information processing at some level of the functional architecture.

To this end, we employed a delayed match-to-category task that contained inherently "supramodal" categories whose members were frequency-modulated (FM) sweeps of different sensory modalities. A given trial contained two stimuli (S1 and S2) separated by a short delay, and the participant was instructed to press a button if S2 belonged to the same category as S1 (Figure 3.1A). Participants learned to classify auditory down-sweeps (A↓) and tactile up-sweeps

(T↑) as members of the one category and auditory up-sweeps (A↑) and tactile down-sweeps (T↓) as members of another category (Figure 3.1B and C). The advantages of this paradigm are threefold: disentanglement of the eventual motor response (Freedman & Assad 2006), task-relevant equation of the sensory modalities, and dissociation of the abstract category from the natural "up vs. down" semantics potentially evoked by a single FM sweep stimulus.

Using functional magnetic resonance imaging (fMRI) and multivariate pattern analysis (MVPA; Haxby et al. 2001), we aimed to uncover which regions of the brain, if any, contained such supramodal information within their local patterns of activity. With this strategy, we hope to take investigations of perceptual decision making one step further by touching upon mechanisms that may be truly flexible with respect to the information that they process.

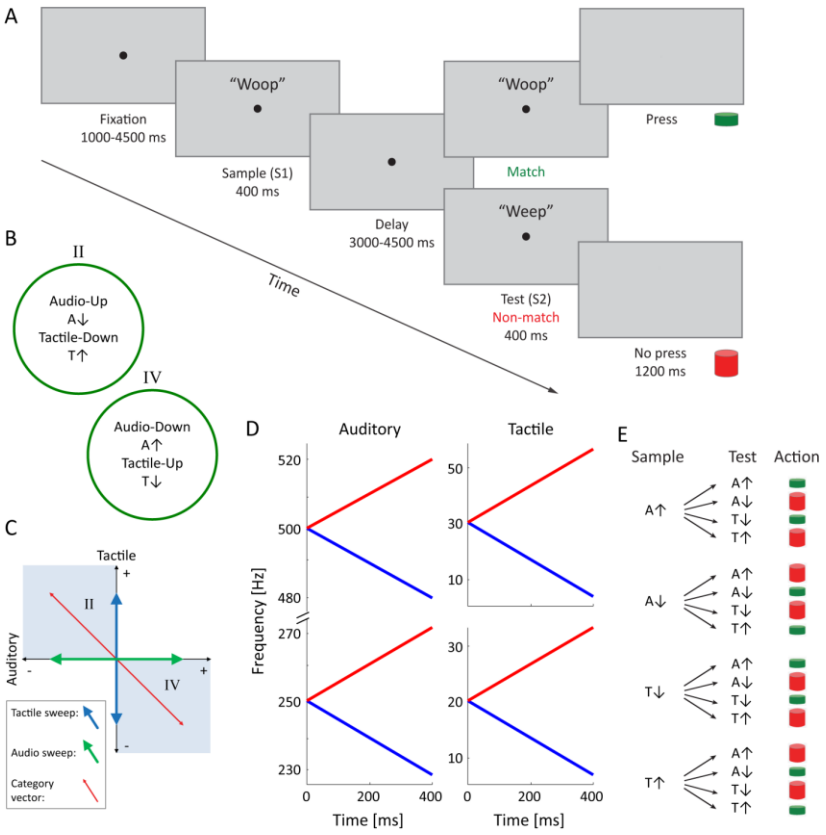


Figure 3.1. Trial protocol and stimulus categories

**(A)** Example trial of the delayed match-to-category task. 'Weep' and 'woop' depict up- and down-sweeps. The fixation dot remained hidden during the intertrial interval (1000–3250 ms). **(B)** Intuitive definition of the arbitrary categories that participants learned prior to the experiment. The category names "II" and "IV" derive from **(C)** a geometric definition of the stimuli and categories (see Stimulus categories). **(D)** A visual representation of the FM-sweep stimuli used in the experiment (see Auditory and tactile stimuli). **(E)** A simple decision tree portraying the 16 possible trial types (ignoring stimulus' initial frequency) and their correct behavioral outcomes.

# MATERIALS AND METHODS

## PARTICIPANTS AND EXPERIMENTAL SESSIONS

Twenty-nine (18 females and 11 males, ~28±7 (μ±σ) years old) healthy subjects participated in the experiments after providing written consent. All procedures followed safety guidelines for MRI research in the Laboratory for Functional Neuroimaging at the Center for Mind/Brain Studies (CIMeC) and were approved by the ethics committee of the University of Trento. Eight participants' datasets were removed from analyses due to poor task performance (range(d') =

[0.38, 0.83]), as determined by a *k*-means clustering algorithm, which systematically clustered these eight participants d's together using a *k* of 4, 5, 6, and 7.

## EXPERIMENTAL PROTOCOL AND DESIGN

A given trial (Figure 3.1A) of the task contained a jittered, pre-stimulus fixation dot of 1000-4500 ms (geometrically distributed, p = 0.2), followed by a 400 ms sample sweep (S1), and then a jittered delay of 3000-4500 ms (geometrically distributed, p = 0.2), followed by a 400 ms test sweep (S2), after which the participant had to press a button with the right index finger if S2 was a member of the same category as S1; otherwise, no motor act was performed. There was a jittered, intertrial interval of 1000-3250 ms (uniformly distributed, in steps of 750 ms) during which the fixation dot disappeared.

The experiment was a rapid, event-related design that followed a factorial structure of 2 (S1 modality: auditory, tactile) × 2 (S1 frequency: high, low) × 2 (S1 direction: down, up) × 2 (S2 modality: auditory, tactile) × 2 (S2 frequency: high, low) × 2 (S2 direction: down, up). Trial presentation was pseudorandomized, and trials containing identical initial frequencies for both S1 and S2 were removed. Each condition was repeated once per run, resulting in a given run containing 48 trials.

## AUDITORY AND TACTILE STIMULI

The frequency sweeps were created using MATLAB (The Mathworks, Natick, MA, USA). Each sweep $\vec{y}$ was generated following the equation

$$\vec{y} = sin(2\pi\vec{f} * \vec{t})$$

where $\vec{f}$ is a vector of a sweep's frequency at a given time point, $\vec{t}$ is a 400 ms vector sampled at 44.1 kHz (aud) or 1Khz (tac), and $\vec{f} * \vec{t}$ is the element-wise product of vectors $\vec{f}$ and $\vec{t}$. Each sweep's initial frequency ($f_0$) at $t_0$ was 250 Hz (aud low), 500 Hz (aud high), 25 Hz (tac low), or 35 Hz (tac high), which was pseudorandomized across trials. The sweeps' final frequencies at $t_{400}$ were $f_0$ ± 20 Hz (aud) and $f_0$ ± 13 Hz) ‖ 23 Hz (tac low ‖ tac high, respectively). All auditory stimuli had a 5 ms rise/fall amplitude envelope. Refer to Figure 3.1D for a visual depiction of the stimuli.

## STIMULUS CATEGORIES

The two task-relevant categories that participants learned were designed to equate sensory modalities, sweep directions, and initial frequencies, such that the category boundary abstracted away from all three of these features. One category (category II) contained auditory down-sweeps and tactile up-sweeps, while the other (category IV) contained auditory up-sweeps and tactile down-sweeps (Figure 3.1B).

The naming scheme derives from a geometric definition of these abstract categories, whereby one maps the two sensory modalities onto a Cartesian plane: auditory on the abscissa and tactile on the ordinate (Figure 3.1C). Vectors projecting from the origin along either of the two axes represent auditory or tactile sweeps, and their signs (i.e., +/−) determine the sweeps directions (up/down). Two additional vectors that project from the origin into quadrants II and IV (at 135° and 315°, respectively) represent the two categories: hence the names II and IV. Thus, a stimulus ($s$) is a member of a particular category ($c$) when the cosine of the angle between vectors $\vec{s}$ and $\vec{c}$ ($\theta_{\vec{s}\vec{c}}$) produces a positive value, or mathematically

$$sgn(\cos\theta_{\vec{s}\vec{c}}) > 0 \rightarrow s \in c$$

## STIMULUS PRESENTATION

Auditory, tactile, and visual stimulation were carried out using ASF (Schwarzbach 2011), built on the Psychophysics toolbox (Brainard 1997) for MATLAB. Visual stimuli (black fixation dots on a gray background) were projected behind participants in the MR scanner onto a semitransparent screen by means of an LCD projector (Epson EMP 9000) at a frame rate of 60 Hz and a resolution of 1280 × 1024 pixels and were viewed via a mirror positioned above the head coil. Auditory stimuli were presented binaurally through MR-compatible headphones (SereneSound, Resonance Technology, Northridge, CA, USA). Tactile stimuli were presented to the tip of the left index finger using a piezoelectric stimulator (Piezostimulator, QuaeroSys, Schotten, Germany), which contained a 2 × 4 matrix of pins (each 1 mm in diameter) that could protrude from a flat surface measuring 4 mm × 8 mm.

## NEUROIMAGING DATA ACQUISITION

Data acquisition was carried out using a 4T Bruker MedSpec Biospin MR scanner and an 8-channel birdcage head coil. Functional images were acquired with a T2*-weighted gradient-recalled EPI sequence. At the beginning of each run we acquired a Point Spread Function (PSF) scan in order to reduce distortion in regions of high-field inhomogeneity (Robinson & Jovicich 2011, Zaitsev et al. 2004). We acquired 32 slices per volume in ascending interleaved order with a repetition time (TR) of 2250 ms (voxel resolution: 3-$mm^3$, in-plane, echo time (TE): 33 ms, flip angle (FA): 75°, gap-size: 0.45 mm). Of the 21 participants whose datasets entered into neuroimaging analyses (see Participants and experimental sessions), 1 completed 7 runs of the experiment, 16 completed 6 runs, 3 completed 5 runs, and 1 completed 4 runs (as a result of time constraints or fatigue/discomfort).

For coregistration of the functional images to high-resolution anatomical images, we acquired a T1-weighted scan using a Magnetization-Prepared Rapid Gradient Echo sequence (MP-RAGE, 176 axial slices, field of view 256mm x 224mm, 1-$mm^3$ isotropic voxels, Generalized Autocalibrating Partially Parallel Acquisition (GRAPPA) with acceleration factor = 2, TR = 2700 ms, TE = 4.180 ms, TI = 1020 ms, FA = 7°) for each participant.

## BEHAVIORAL DATA ANALYSIS

Resampling tests were used to generate null distributions from the behavioral data in order to determine if group-level accuracies for the two categories differed from chance (in addition to potentially differing from each other). For each of the two tests against chance, values from each category were randomly permuted with values from a theoretical distribution of chance-level values (i.e., 50%) and subsequently divided into two pools, from which the test statistic—the difference of the pools' means—was calculated. For the test of category differences, the values for each category were permuted with each other. This procedure was repeated $10^5$ times, resulting in 3 null distributions (one for each test), from which exact p-values were computed as the number of values in the null distribution that were more extreme than the originally observed test statistic divided by the total number of iterations (i.e., $10^5$), adding 1 to both the numerator and denominator (to account for the original dataset being a possible permutation).

## NEUROIMAGING DATA ANALYSIS

Analysis of the acquired neuroimaging data was carried out with Brainvoyager QX 2.8 (Goebel et al. 2006), the Neuroelf software package (Weber, neuroelf.net), and CoSMoMVPA (Oosterhof & Connolly, cosmomvpa.org). Note that only the trials in which participants correctly categorized the stimuli were included in the neuroimaging analyses.

## PREPROCESSING

The acquired PSF data were used to apply distortion correction to the EPI images (Zaitsev et al. 2004). Next, the first three volumes of each functional scan were discarded to account for signal saturation. Preprocessing of the functional data included, in the following order, slice time correction (cubic spline interpolation), motion correction with respect to the first (remaining) volume in the first run (estimation with trilinear, resampling with sinc interpolation), and temporal highpass filtering (cutoff: 3 cycles within the run). For each participant, functional data were then co-registered to high-resolution, de-skulled anatomical scans in native space; subsequently, echo-planar and anatomical volumes were transformed into standardized space (Talairach & Tournoux 1988).

## CORTEX BASED ALIGNMENT

Due to high variability in cortical anatomy between subjects, we performed a cortex-based alignment in an effort to increase the accuracy of the localization of effects at the group-level (Fischl et al. 1999). The cortical surface of each participant was segmented from the rest of the brain, and the resulting mesh surface was morphed into a sphere, after which the gyral/sulcal folding pattern was aligned to a group-average template sphere. The transformation matrices that resulted from this alignment were then applied to each participant's functional data, such that further group-level statistics could be carried out on a standard 2D cortical surface constructed from all participants.

## UNIVARIATE ANALYSIS

Data were analyzed with a random-effects (RFX) general linear model (GLM). Regressors of interest, which were all combinations of features for S1 (i.e., aud/tac × up/down; collapsed

across $f_0$), all combinations of features for S2 (i.e., aud/tac × up/down; collapsed across $f_0$), the onset of the fixation dot, and the button press (whose onset was calculated from the reaction time), were modeled with a dual-gamma hemodynamic response function (HRF; onset = 0, time to peak = 5 s, dispersion = 1, undershoot ratio = 6, undershoot peak = 15 s, undershoot dispersion = 1). Motion correction parameters for 6 directions (3 translational, 3 rotational) were modeled as regressors of non-interest.

## MULTIVARIATE PATTERN ANALYSIS

Conditions of interest (e.g., II and IV) for a surface-based searchlight analysis (Kriegeskorte et al. 2006, Oosterhof et al. 2011) were selected, and single-trial GLMs were computed in volume space to produce maps of the resulting beta-weights' t-scores using the same parameters as in the previous GLM computation for the univariate analysis. These volume maps were sampled using the surfing toolbox (Oosterhof et al. 2011) in order to morph the functional data into surface maps, which were then passed to a linear discriminant analysis (LDA) classifier implemented with CoSMoMVPA. The LDA attempted to classify the two conditions based on the pattern of t-scores across the vertices of the searchlight (r = 8 mm, 12 mm). Training/testing of the LDA followed a leave-one-run-out cross-validation procedure, and classification accuracy was computed for each permutation of the cross-validation. The resulting classification accuracy for a given vertex was the mean of the all the permutations' accuracies. This process was repeated at each vertex of the map. Accuracies were then converted to d'-values, and a 1-nearest neighbor smoothing kernel was applied to individual participants' d' maps before running group-level statistics.

With respect to the cross-decoding analysis (i.e., training on A↓ vs. A↑; testing on T↑ vs. T↓), rather than applying a leave-one-run-out cross-validation scheme, all the training data

patterns were lumped together from all runs, and all the test data patterns were lumped together from all runs (and vice versa) for a given participant before applying a 2-fold cross-validation scheme. In short, having four experimental conditions of interest, we trained on 1 vs. 2, tested on 3 vs. 4, obtained classification accuracies, then trained on 3 vs. 4, tested on 1 vs. 2, obtained classification accuracies, and finally averaged the two sets of accuracies in order to obtain a single classification accuracy for a given vertex.

## MULTIPLE-COMPARISONS CORRECTION

To correct for multiple comparisons, we employed threshold-free cluster-enhancement (TFCE; Smith & Nichols 2009) as it is implemented in CoSMoMVPA with default parameters ($h_0 = 0$, E = 0.5, H = 2, dh = 0.1). CoSMoMVPA then followed a bootstrapping procedure, in which the sign of a participant's d' map was flipped with a probability of 0.5, the t-test across participants was performed, each vertex's TFCE score was computed, and the resulting map's largest TFCE score was stored. This process was repeated $10^4$ times, resulting in a null distribution of $10^4$ TFCE scores. Vertices of the surface mesh pertaining to subcortical structures were excluded from this analysis using a mask based on the cortical parceling described by Yeo et al. (2011).

## FUNCTIONAL CONNECTIVITY ANALYSIS

Functional connectivity (Friston 2011) was calculated using the nine regions that resulted from the three multivariate analyses. For each participant, the timecourses for all vertices within a region were averaged, and Pearson's correlation was computed across the regions. The resulting 36 correlations were then Fisher transformed, permitting a t-test across participants, in order to determine which regions' correlated activation levels were different from zero.

# RESULTS

## BEHAVIORAL RESULTS

The task proved to be challenging as participants performed on average (± S.E.M.) at 73.4 (± 3.88) % for category II and 66.2 (± 3.69) % for category IV. Nevertheless, participants performed better than chance ($p = 9.9 \times 10^{-6}$; $p = 3.0 \times 10^{-5}$: II and IV, respectively), while performance appeared not to differ between the two categories ($p = 0.09$), as revealed by resampling procedures (see Behavioral data analysis). Overall mean task sensitivity ($\pm\sigma$) was 2.2 ($\pm$0.8).

## NEUROIMAGING RESULTS

### TASK ELICITS GENERAL BOLD CHANGE ACROSS A DISTRIBUTED NETWORK; NO DIFFERENCE BETWEEN ABSTRACT CATEGORIES

To seek out regions that were generally involved in the delayed match-to-category task, we computed the mass-univariate conjunction of all S1 regressors with all S2 regressors. Correcting for multiple comparisons using threshold-free cluster enhancement (TFCE) yielded a variety of regions whose BOLD signal change survived the threshold of $p_{FWER} < 0.01$ (Figure 3.2, Table 3.1). While the bilateral superior temporal gyrus (STG) and right parietal operculum (Par Op) yielded up-regulated BOLD signal, we observed down-regulated BOLD signal in the bilateral medial frontal gyrus (MedFG) and the right anterior cingulate gyrus (ACC).

However, computing the mass-univariate contrast of category II vs. category IV, conjoining S1 and S2 regressors (i.e., [S1II > S1IV] ∩ [S2II > S2IV]) resulted in no voxels

surviving any acceptable threshold following whole-hemisphere multiple comparisons correction (LH: $p_{TFCE} > 0.33$; RH: $p_{TFCE} > 0.34$).

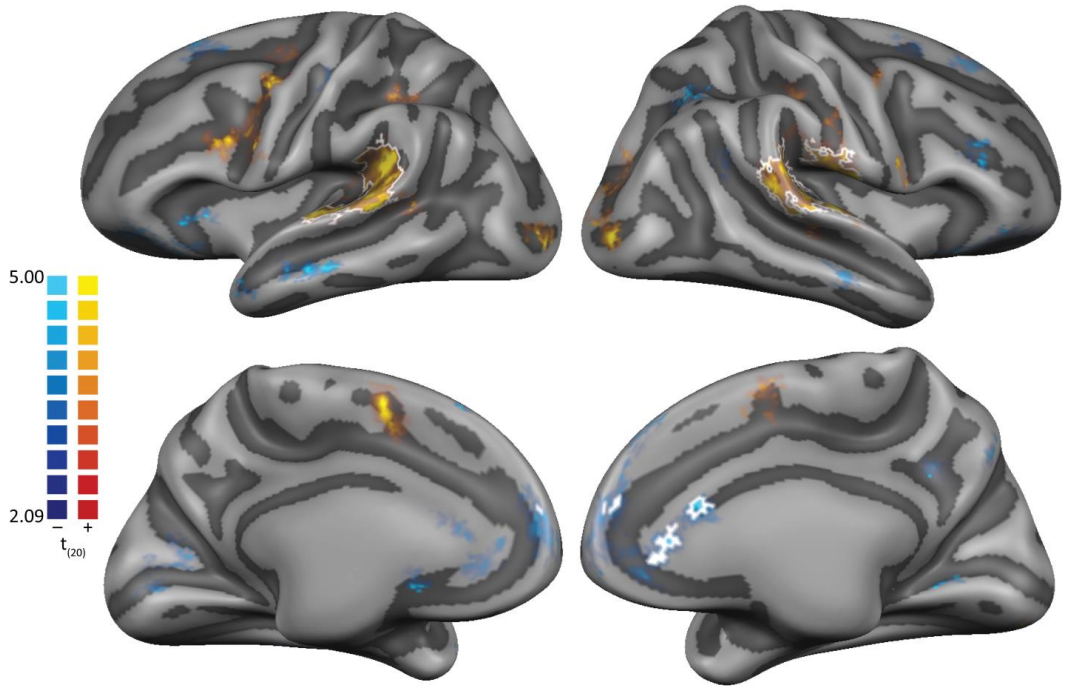


Figure 3.2. Univariate results

Uncorrected (from $p < 0.05$) group-level t-scores of activation revealed by the conjunction [S1 ∩ S2] visualized on a partially-inflated, cortex-based aligned, group-average brain. Transparency scales with the magnitude of the t-score. White contours represent regions whose TFCE scores survived a multiple-comparisons correction ($p_{TFCE} < 0.01$, FWER).

| Region | Hemisphere | Peak Tal. coords. (x, y, z) | Vertex count | TFCE p-value | t-score | p-value |
|---|---|---|---|---|---|---|
| STG/PT | L | (-47, -40, 18) | 972 | $2.0 \times 10^{-4}$ | 4.92 | $8.2 \times 10^{-5}$ |
| MedFG | L | (-9, 50, 23) | 3 | $3.0 \times 10^{-3}$ | -5.96 | $8.0 \times 10^{-6}$ |
| STG | R | (56, -28, 11) | 950 | $2.0 \times 10^{-4}$ | 6.15 | $5.0 \times 10^{-6}$ |
| Par Op | R | (49, -14, -16) | 357 | $7.0 \times 10^{-4}$ | 5.42 | $2.6 \times 10^{-5}$ |
| ACC | R | (5, 23, 22) | 45 | $3.9 \times 10^{-3}$ | -4.45 | $2.5 \times 10^{-4}$ |
| MedFG | R | (11, 44, 22) | 7 | $6.2 \times 10^{-3}$ | -5.97 | $8.0 \times 10^{-6}$ |

Table 3.1. Regions obtained from the univariate analysis

Descriptive statistics of the six regions depicted in Figure 3.2. Regions are abbreviated as superior temporal gyrus/planum temporale (STG/PT), medial frontal gyrus (MedFG), parietal operculum (Par Op), anterior cingulate cortex (ACC). Coordinates refer to the location of the peak t-score within a cluster.

## TASK-RELEVANT CATEGORIES ENCODED IN A RIGHT-LATERALIZED NETWORK

In order to determine which brain regions encoded the supramodal categories that participants learned for the task, we trained and tested a linear discriminant analysis (LDA) classifier on patterns of activity from stimuli that pertained to category II (A↓ and T↑) vs. category IV (A↑ and T↓). A searchlight analysis revealed a variety of regions (Figure 3.3A, Table 3.2), all lateralized to the right hemisphere, from which the LDA could decode these categories better than chance following TFCE-based, multiple-comparisons correction ($p_{FWER} < 0.01$)

## SUPRAMODAL CONCEPT OF "UP VS. DOWN" LOCALIZED TO LEFT ASSOCIATION CORTEX

Additionally, we sought to reveal cortical representations of "up" and "down" independent of the sensory modality and the task-relevant category. To this end, we split the data in an "orthogonal" manner to the II vs. IV analysis, by training and testing the LDA on patterns of activity from category I (A↑ and T↑) vs. category III (A↓ and T↓). Surprisingly, the LDA very strongly decoded this information in only the parietal-temporal-occipital junction (PTOJ) of the left hemisphere ($p_{FWER} < 0.01$; Figure 3.3B, Table 3.3).

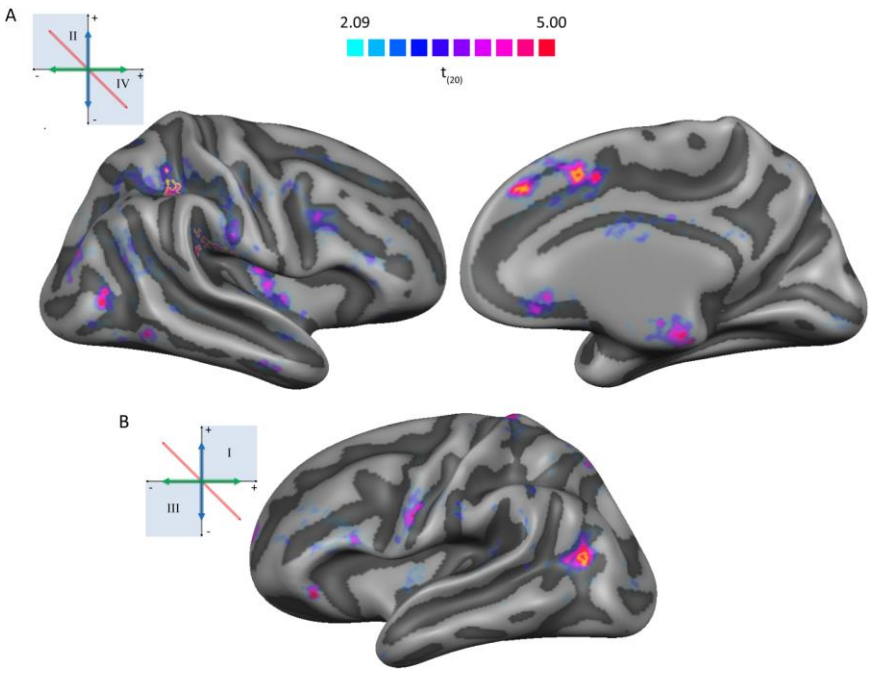


Figure 3.3. Multivariate results

Uncorrected (from $p < 0.05$) group-level t-scores of LDA classification of **(A)** II vs. IV (i.e., learned categories) and **(B)** I vs. III (i.e., supramodal up-vs. down-sweeps). In both cases, transparency scales with the magnitude of the t-score, and yellow contours depict regions whose TFCE scores survived a multiple-comparisons correction ($p_{TFCE} < 0.01$, FWER).

| Region | Peak Tal. coords. (x, y, z) | Vertex count | TFCE p-value | Decoding d' (% correct) | t-score | p-value |
|---|---|---|---|---|---|---|
| IPS | (34, -41, 37) | 110 | $5.1 \times 10^{-3}$ | 0.14 (52.75) | 4.68 | $1.4 \times 10^{-4}$ |
| Par Op | (48, -27, 22) | 97 | $6.0 \times 10^{-3}$ | 0.09 (51.91) | 4.21 | $4.3 \times 10^{-4}$ |
| pIns | (46, -35, 19) | 61 | $4.3 \times 10^{-3}$ | 0.10 (52.00) | 4.90 | $8.7 \times 10^{-5}$ |
| MedFG | (8, 10, 44) | 10 | $5.8 \times 10^{-3}$ | 0.12 (52.37) | 6.03 | $7.0 \times 10^{-6}$ |
| aMedFG | (8, 29, 40) | 5 | $7.6 \times 10^{-3}$ | 0.09 (51.86) | 6.46 | $3.0 \times 10^{-6}$ |
| SPL | (27, -45, 46) | 3 | $9.6 \times 10^{-3}$ | 0.10 (51.96) | 4.52 | $2.1 \times 10^{-4}$ |

Table 3.2. Regions obtained from the multivariate analysis of category II vs. category IV

Descriptive statistics of the six right hemisphere regions depicted in Figure 3.3A. Regions are abbreviated as intraparietal sulcus (IPS), parietal operculum (Par Op), posterior insula (pIns), [anterior] medial frontal gyrus ([a]MedFG), and superior parietal lobule (SPL). Here coordinates also refer to the location of the peak t-score within a cluster.

| Region | Peak Tal. coords. (x, y, z) | Vertex count | TFCE p-value | Decoding d' (% correct) | t-score | p-value |
|---|---|---|---|---|---|---|
| PTO Junction | (-40, -65, 13) | 18 | $2.8 \times 10^{-3}$ | 0.14 (52.75) | 7.26 | $1.0 \times 10^{-6}$ |

Table 3.3. Regions obtained from the multivariate analysis of category I vs. category III

Descriptive statistics of the single, left hemisphere region depicted in Figure 3.3B. Same conventions as in Table 3.2.

## PRECUNEUS AND POSTERIOR INSULA REPRESENT CATEGORY MEMBERS SIMILARLY ACROSS MODALITIES

Crucially, we aimed to uncover from which regions of the brain, if any, information from one modality could be decoded from information of another modality. Thus, we trained an LDA classifier on between-category auditory-sweeps and tested on the corresponding within-category tactile sweeps (i.e., train on A↓ vs. A↑; test on T↑ vs. T↓), and vice versa. This searchlight analysis revealed that such cross-modality information was encoded in the left posterior insula and the left precuneus ($p_{FWER} < 0.05$; Figure 3.4, Table 3.4).

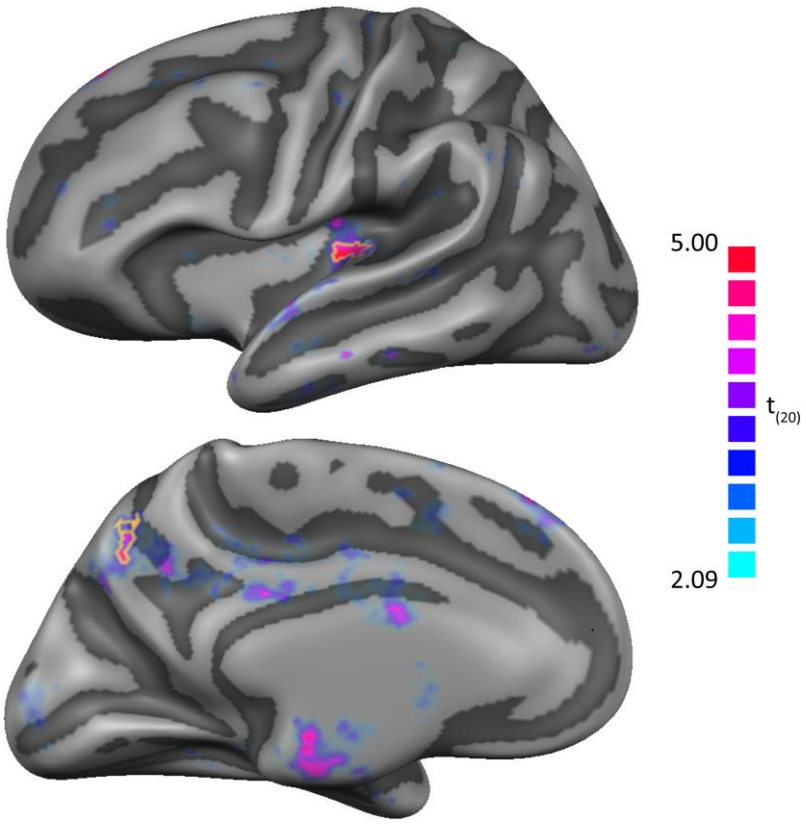


Figure 3.4. Cross-modality decoding results

Uncorrected (from $p < 0.05$) group-level t-scores of LDA classification of category-membership across different modalities. In short, the LDA was trained on A↓ vs. A↑ and then tested on T↑ vs. T↓, and vice versa. Again, transparency scales with the magnitude of the t-score, and yellow contours depict regions whose TFCE scores survived a multiple-comparisons correction ($p_{TFCE} < 0.05$, FWER), showing that truly supramodal information is present and decodable within the posterior insula and precuneus of the left hemisphere.

| Region | Peak Tal. coords. (x, y, z) | Vertex count | TFCE p-value | Decoding d' (% correct) | t-score | p-value |
|---|---|---|---|---|---|---|
| pIns/Claustrum | (-40, -65, 13) | 83 | $1.0 \times 10^{-2}$ | 0.11 (52.21) | 5.64 | $1.6 \times 10^{-5}$ |
| Precuneus | (-6, -66, 7) | 49 | $3.0 \times 10^{-2}$ | 0.12 (52.40) | 4.82 | $1.0 \times 10^{-4}$ |

Table 3.4. Regions obtained from the cross-modality decoding analysis

Descriptive statistics of the regions depicted in Figure 3.4. Same convention as in Table 3.2

## RELATIVELY STRONG FUNCTIONAL CONNECTIVITY BETWEEN POSTERIOR REGIONS, BUT NOT FRONTAL REGIONS

To assess the level of potential communication among the regions obtained from these three multivariate analyses, we performed a follow-up functional connectivity analysis. Despite the regions carrying different information, functional connectivity can allow us to infer potential commonalities in information processing. The group-level analysis (Figure 3.5, Table 3.5) revealed stronger connectivity predominantly among the posterior regions ($t_{(19)} > 2.54$, $p < 0.01$) and, interestingly, not within the frontal regions ($t_{(19)} < 2.2$, $p > 0.02$).

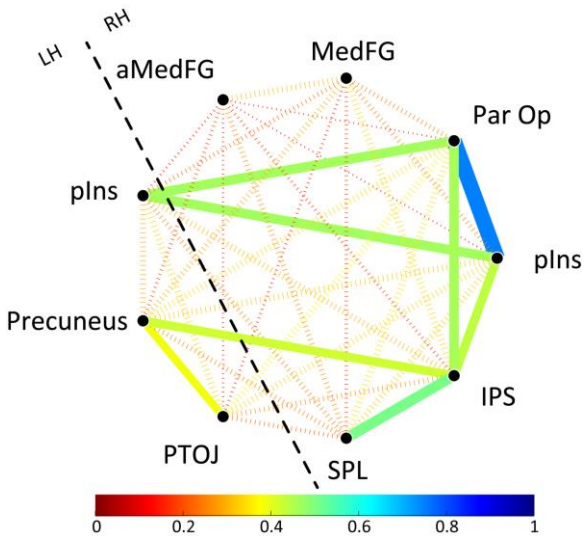


Figure 3.5. Functional connectivity results

Group-level, correlation-based functional connectivity from the nine regions revealed by the three multivariate analyses. Edge color scales with the value of Pearson's r, and edge thickness scales with the magnitude of the t-score. Unbroken edges are those that survived a statistical threshold of $p < 0.01$. See table 5 for regions that correspond to each abbreviation.

| Network edge | Pearson's r | t-score | p-value |
|---|---|---|---|
| Pos Ins (RH), Par Op | 0.75 | 13.27* | $2.3 \times 10^{-11}$ |
| SPL, IPS | 0.51 | 4.53* | $1.1 \times 10^{-4}$ |
| Pos Ins (RH), Pos Ins (LH) | 0.47 | 3.80* | $6.1 \times 10^{-4}$ |
| Par Op, Pos Ins (RH) | 0.46 | 3.78* | $6.3 \times 10^{-4}$ |
| Par Op, IPS | 0.46 | 3.74* | $6.9 \times 10^{-4}$ |
| Pos Ins (RH), IPS | 0.44 | 3.41 | $1.5 \times 10^{-3}$ |
| Precuneus, IPS | 0.42 | 3.20 | $2.4 \times 10^{-3}$ |
| Precuneus, PTO Junction | 0.37 | 2.74 | $6.5 \times 10^{-3}$ |

Table 3.5. Functional connectivity

Descriptive statistics pertaining to the edges of the group-level functional connectivity analysis that survived a statistical threshold of $p < 0.01$. Asterisks in the t-score column indicate edges that also survived the Bonferroni threshold ($t_{(19)} < 3.43$, $p_{Bonf} < 0.0014$). Regions are abbreviated as follows: posterior insula (Pos Ins), parietal operculum (Par Op), superior parietal lobule (SPL), intraparietal sulcus (IPS), parietal-temporal-occipital (PTO). Where necessary, the hemisphere to which the region belongs is denoted in parentheses.

## DISCUSSION

By employing a novel paradigm, in which auditory and tactile information were abstractly equated, we were able to investigate which regions of human cortex carried high-level information that abstracted away from the sensory modality during perceptual decision making. Using a whole-brain multivariate searchlight and three distinct manners of partitioning the neuroimaging data, a linear discriminant classifier analysis decoded the learned supramodal categories, the concept of "up/down", and supramodal category membership from a variety of non-overlapping brain regions. Entering these regions into a follow-up functional connectivity analysis revealed a higher degree of communication between and within the parietal and insular regions, but not the frontal regions. In addition to revealing cortical representations of supramodal information, this connectivity pattern suggests a functional distinction in the information processing stream between the posterior and anterior regions.

While our standard mass-univariate analysis exposed brain regions that are commonly associated with such perceptual tasks (Duncan 2010, Fedorenko et al. 2013, Woolgar et al. 2011), one region in particular, the right parietal operculum, both activated for the task and

carried category-level information. It is thus possible that the parietal operculum play a more general role in the processing of auditory and tactile information, as past work has demonstrated auditory stimuli activated secondary somatosensory neurons in monkeys (Lemus et al. 2010).

Previous work has shown the involvement of parietal cortex in representing high-level abstract information (Freedman & Assad 2006, Hebart et al. 2012, Rishel et al. 2013, Wurm & Lingnau 2015), and the present results corroborate our earlier claim that the right IPS encodes category-level information (Levine and Schwarzbach, *under review*). Although the current results demonstrate category-level information represented more anteriorly along the IPS than in our previous study, the task employed in our earlier experiments only required participants to make unimodal perceptual judgments, whereas the current study entails a supramodal decision. Thus, the cognitive functions employed to carry out these two tasks may have been slightly different and potentially represented in distinct parts of the IPS.

Moreover, the current experimental design allowed us to explore representations of supramodal information more thoroughly than in previous studies. From this, we showed that the parietal-temporal-occipital junction (PTOJ: a.k.a. TPOJ) represents the semantic concept of "up" and "down" irrespective of the stimulus' sensory modality and of the task-relevant categories. The PTOJ has been implicated in a slew of cognitive functions including language (Duffau et al. 2005), symbolic processing (Holloway et al. 2010), and working memory (Deprez et al. 2013) and has been considered an ideal hub for multimodal integration (Hubbard & Ramachandran 2005) due to its location and complex structural connectivity (De Benedictis et al. 2014). Additionally, the PTOJ is only slightly posterior to the lateral occipitotemporal cortex, a region that has recently been postulated to contain high-level representational spaces for a wide variety of cognitive functions (Lingnau & Downing 2015). Considered together, these

various perspectives provide evidence for the general area around the PTOJ (and its underlying white matter tracts) in potentially representing abstract information in a very general framework, irrespective of a stimulus' original sensory modality and the relevant task at hand.

Most critically, however, we performed a cross-*modality* decoding analysis, a suggestion brought up by Goebel and van Atteveldt (2009), through which we showed that the precuneus and posterior insula of the left hemisphere contain similar patterns of information across the auditory and tactile modalities. Previously, activity in the posterior insula has been implicated in "crossmodal matching" (Calvert 2001) and generally considered as a multimodal zone for merging sensory information (Chang et al. 2013), while activity in the precuneus has been linked to such tasks as attentional switching for different sensory modalities (Shomstein & Yantis 2004, Yantis et al. 2002), multimodal detection (Langner et al. 2012), and supramodal goal-recognition (Spunt & Lieberman 2012). Our results, however, extend the knowledge of these regions by demonstrating not only that they contain information specific to category membership, but that the representations of such information can likely be considered supramodal. It is possible that underlying these regions are cognitive resources that can flexibly engage regardless of the information's original sensory modality.

Interestingly, for the most part, our analyses did not reveal supramodal information encoded in regions of the frontal lobes, despite various regions in the prefrontal cortex being implicated in crossmodal/supramodal behavior (Klemen & Chambers 2012). The results of our functional connectivity analysis seem to suggest a functional split between the parietal and frontal supramodal regions, as most of the parietal areas revealed by the multivariate analyses correlated with one another, but the frontal areas did not. Taking into account our experimental design, which disentangled the motor response from the stimulus categorization and collapsed the category-level information across many dimensions, one possible explanation is that the

parietal and insular lobes may predominantly represent specific high-level (or categorical) abstract information, especially that which may be considered supramodal. Thus, the medial frontal gyrus, which has been shown to have to activate when multiple stimulus modalities are contextually congruent (Laurienti et al. 2003), may represent amodal information necessary for conflict resolution, such that motor-related processes can engage at a later stage of the functional architecture.

In conclusion, by ensuring that supramodal processing must take place somewhere along the information processing stream, we demonstrated that 1) supramodal category-level information can be decoded from the right intraparietal sulcus, parietal operculum, posterior insula, and medial frontal gyrus, 2) a supramodal semantic concept of "up vs. down" is carried very focally in the parietal-temporal-occipital junction, and, most crucially, 3) category membership can be decoded across sensory modalities in the left posterior insula and precuneus. We believe that these results highlight the role of the parietal and insular cortices in abstractly representing high-level information during perceptual decisions, with an emphasis on potentially being loci of supramodal cognitive functions.

# 4. A NEW PERSPECTIVE FOR PERCEPTUAL DECISION MAKING

## RECAPITULATION

The experiments described in this dissertation aimed to bring a new perspective into the studying of perceptual decision making by better understanding where in the human brain is non-visual information pertinent to the categorization process represented. The driving force behind this line of research sought namely to investigate the idea that effects often observed in regions of the frontal lobe (Binder et al. 2004, Heekeren et al. 2004, Philiastides et al. 2011, Pleger et al. 2006, Preuschhof et al. 2006) may be more concerned with eventual motor responses and cognitive control (Koechlin et al. 2003), whereas the parietal lobes (Freedman & Assad 2006, Hebart et al. 2012, O'Connell et al. 2012, Ploran et al. 2007, Rishel et al. 2013) may play a more fundamental role in abstraction during categorization. Many paradigms used to investigate mechanisms of perceptual decision making either failed to disentangle the motor act from the stimulus categorization and/or always resulted in some form of motor act. By knowing that motor processes will certainly engage *at some point* during a given task, it is unclear which cognitive processes associated with motor and pre-motor activity may consequently stay online, adding a series of potential confounding factors when interpreting observed effects within the framework of perceptual decision making.

Moreover, the field of perceptual decision making has been dominated by investigations using the visual modality, which naturally led the progression of our line of research toward studying the auditory and tactile systems. Ultimately, though, one of the more interesting facets of perceptual decision making is whether its underlying mechanisms are modality-general rather than specific for each sensory modality. To this end, we wanted to not only supply the

field with auditory and tactile studies but also to look more deeply into the idea of modality-general, or supramodal, cortical representations of information.

While previous work has looked into the idea of supramodal representations of information using conjunction analyses (Beauchamp et al. 2004, van Atteveldt et al. 2004), the key result of our finding from chapter two is not whether the information represented in the right intraparietal sulcus is supramodal but rather the simple fact that such information seems not to be represented within the frontal lobes. Studies that have attempted to disentangle the motor response from the stimulus categorization have reported effects in parietal regions (Filimon et al. 2013, Hebart et al. 2012), which we also find using an audiotactile conjunction analysis, lending credence to the idea that the parietal lobes, regardless of the extent to which information processing therein is supramodal, carry abstract, task-relevant information during perceptual decisions.

The experiment described in chapter three was expressly designed to dig deeper into the question of supramodal information representation within the cortex. Although prior work has made use of repetition suppression in an attempt to uncover supramodal representations (Tal & Amedi 2009, van Atteveldt et al. 2010), it has been argued that neither conjunction analyses nor repetition suppression are sufficient for claiming supramodality (Goebel & van Atteveldt 2009). Rather, the cross-modal decoding analysis we performed in the second experiment was essentially the strongest suggestion that Goebel and van Atteveldt (2009) put forth as a means of testing for supramodality. While the other decoding analyses we performed do contain supramodal stimuli, at most their results can build a modality-independent framework around the ideas that abstract concepts are represented within the right parietal lobe (Wurm & Lingnau 2015) and that semantics are represented in the vicinity of the left angular gyrus (Fairhall & Caramazza 2013). This limitation is due to the nature of the LDA

training/testing procedure we utilized for these analyses, which did not allow us to claim that the underlying processing is supramodal to the same extent as in the cross-modal decoding analysis. In essence, the cross-modal decoding analysis is the only analysis in which the LDA classifier's decision boundary obtained from the training phase on one modality is directly tested on a different modality (Figure 4.1), implying that information from both modalities is similarly separable in a high-dimensional space and therefore similarly represented along those dimensions. It is for this reason that I focus predominantly on the representations within the precuneus and posterior insula when discussing supramodal representations from this experiment.

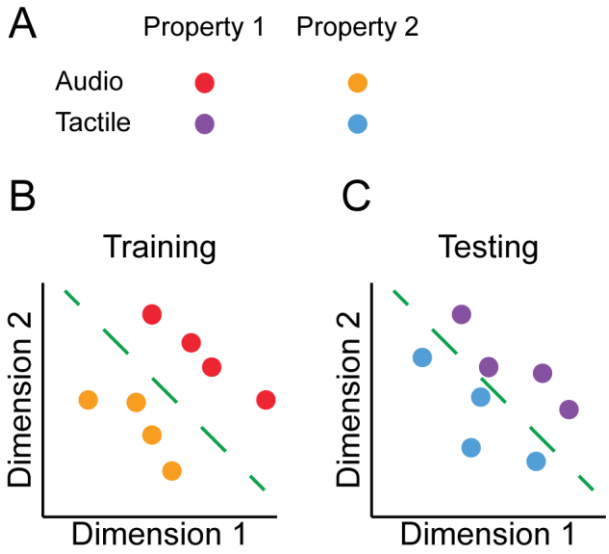


Figure 4.1. Cross-modal separability as a criterion for supramodality

**(A)** Given data from two sensory modalities with two arbitrary properties in an n-dimensional space, **(B)** training a machine learning algorithm to discriminate the two properties from one modality yields a decision boundary that can be used to **(C)** test whether the same properties from the other modality are separable with the same decision boundary. This is a crucial use of multivariate analyses for truly gauging the extent to which abstract representations of information may be considered supramodal (Goebel & van Atteveldt 2009).

One observation worth noting is the seeming discrepancy between the results of the second and third chapters. At first glance it appears that category-level information in the first experiment is represented more posteriorly along the intraparietal sulcus than the category-

level information representations revealed in the second experiment. There are three predominant responses to this ostensible inconsistency. First, and as mentioned in chapter three, the task participants engaged in during the first set of experiment was essentially unimodal, while the task participants engaged in during the experiment of chapter three was supramodal. The complexity of the second task with respect to the first can indicate that either a different or more varied set of cognitive processes was necessary for the second task. This difference can potentially require the participation of neurons from distinct aspects of the intraparietal sulcus. Secondly, the types of analyses carried out for the multiple-comparisons corrections were different. When analyzing the data from the first experiment, we obtained our statistical thresholds by performing a cluster-based analysis, whereas later, the threshold-free cluster enhancement technique (Smith & Nichols 2009) was implemented into the software package we were using, and thus we chose to make use of this more sensitive (and less arbitrary) analysis for the second experiment. The differences in analysis choices can lead to different levels of statistical sensitivity. Thirdly, the results obtained from the threshold-free cluster enhancement were quite widespread, and, as such, I chose to present the results of the second experiment at a more conservative threshold ($p < 0.01$, FWER) for purposes of spatial specificity and interpretability. However, when visualizing the results of the multivariate analyses (in the second experiment) at a more relaxed threshold ($p < 0.05$, FWER), one sees that much of the right intraparietal sulcus does in fact carry the supramodal, category-level information. Thus, at least with respect to this particular decoding analysis, the results from the first and second experiments can fall in line with one another.

The interpretations from the two experiments, however, do differ. After completing the first experiment, we conjectured that "the right [intraparietal sulcus] is a categorizer that abstracts away from both the input and output domains". To an extent, this may still be the case,

but I believe the results from experiment two improve our understanding of which regions carry supramodal information. Instead, we can more readily declare that the precuneus and posterior insula abstract away from the input domain, whereas the intraparietal sulcus no longer seems to meet the criteria for necessarily processing information in a supramodal fashion.

## SUPRAMODALITY

The predominant theme that this dissertation has taken on regards the notion of supramodal procession in perceptual decision making. The definition, and even existence, of supramodality within the brain has been more popularly discussed in the field of multisensory integration. Gallese and Lakoff describe supramodality as something that "uses information coming from areas specialised for individual distinct modalities, but is not itself involved in the individual distinct modalities" (2005, p. 459). However, Gallese and Lakoff don't believe in supramodality, and instead subscribe to a notion of multimodality positing that "[m]ultimodality does everything that supramodality has been hypothesised to do, and more" (2005, p. 459), but such fuzziness does not allow us to assess the extent to which both supramodality and multimodality may be present in the cortex. Klemen and Chambers, on the other hand, more recently described a reasonable difference between supramodality and multimodality in that "supramodal brain activation appears to be caused by the stimulation of one sensory modality, or by the simultaneous stimulation of several modalities" (2012, p. 112), while multimodality can describe a region in which unisensory neurons that process information from different modalities are in very close proximity, resulting in the observed epiphenomenon of both neural populations co-activating one another merely as a result of their vicinity.

Although neither the insula nor the precuneus appear in Klemen and Chambers' review of supramodal brain regions (2012), both areas have been documented as being rather complex in that they project to various parts of the brain (Binder & Desai 2011, Cloutman et al. 2012, Margulies et al. 2009, Zhang & Li 2012) and may be sites for multimodal integration (Cavanna & Trimble 2006, Hadjikhani & Roland 1998, Naghavi et al. 2007). However, what we show here for the first time is the similarity in the pattern of information across both sensory modalities in these two regions of cortex. These results from the multivariate pattern analysis have profound implications for how we will eventually characterize the role of the precuneus and posterior insula within the perceptual decision making process. That is, considering theoretical functional architectures underlying perceptual decisions (Figure 4.2), the fact that we find this supramodal information representation in the precuneus and posterior insula (and that we disentangled the participants' eventual motor act from the stimulus categeorization) indicates to us that model A is false; i.e., some supramodal process exists at some point in the functional architecture. Where precisely to place the precuneus and posterior insula within this functional architecture is still unclear. In other words, the exact cognitive function(s) underpinning these regions' neural activity could be categorization (as seen in model B), an earlier function, such as resource allocation (model B'), or even the output of the categorization function itself. If these results represented the output of a categorization function, this would be an interesting case, as one might then argue that the representations output from a supramodal categorization function would likely be amodal, rather than supramodal.

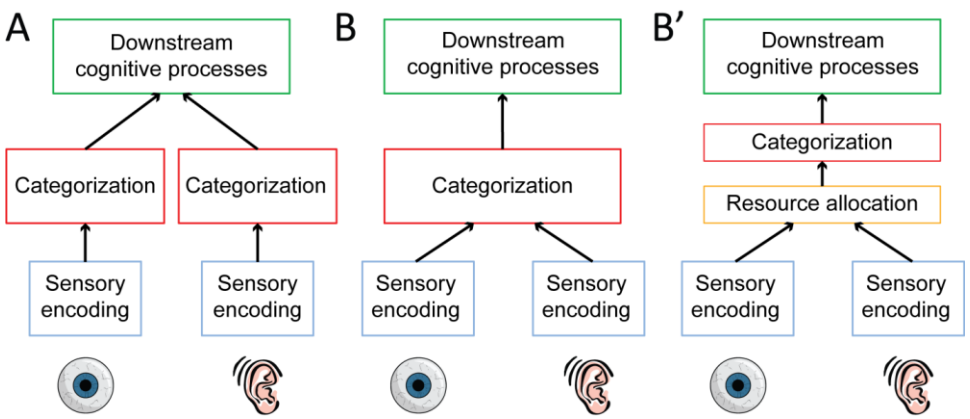


Figure 4.2. Theoretical function architectures

**(A)** A model architecture, which we believe is false, depicting unisensory information being processed entirely in parallel until after categorization has taken place. **(B)** An alternative theory stating that the categorization function itself is the supramodal function which integrates information from various sensory modalities. Given the experiments presented in this dissertation, this architecture is not discernible from another alternative, in which **(B')** earlier possible functions, such as resource allocation, are the supramodal integrators.

Additionally, it is worth noting that the aforementioned model architectures need not be serial. Certain functions, such as resource allocators or information integrators, could very well trigger in parallel to other functions, acting as amodal auxiliary functions that initiate only when necessary (Figure 4.3).

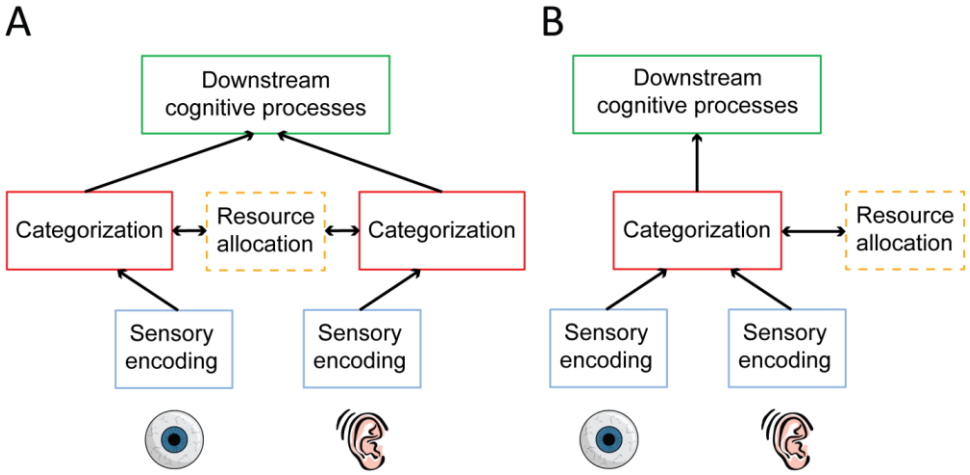


Figure 4.3. Resource allocation as an amodal theoretical function

**(A)** A model architecture, in which sensory information is categorized independently, but a common, modality-free function, such as resource allocation, engages in all cases. **(B)** Another possible architecture, in which categorization is a supramodal function, but resource allocation is an amodal auxiliary function.

Despite the inability to make finer-grained distinctions regarding the previously discussed functional architecture, one interesting addition arises from the results of the functional connectivity analysis of the second experiment (Figure 3.5). The first result to be aware of is the fact that the two frontal (MedFG and aMedFG) regions neither correlate with each other nor with the other regions. This division already allows us to posit that underlying these frontal regions may be cognitive processes that lie further downstream in the functional architecture (e.g., post-hoc error-checking). Secondly, however, one notices that the precuneus and left posterior insula do not correlate, although these were the only two regions that carried "truly" supramodal information, according to the multivariate analyses. This observation suggests that the supramodal cognitive functions housed within these regions are either situated at different levels of the functional architecture and/or dissimilar from one another. Nevertheless, beyond recognizing differences between cortical regions' potential cognitive functions, we still remain unable to theorize more distinctly about the specific functions themselves, which is discussed in further detail in the next section.

## THE BIGGER PICTURE AND FUTURE DIRECTIONS

To put these findings into a larger perspective, one overarching account of the cognitive functions associated with such supramodal brain regions comes from suggestions by Tenenbaum (21 April, 2015) in a keynote lecture, wherein he theorized that the brain contains a "physics engine", similar to those found in modern video games. With respect to video games, physics engines use a set of parameters (usually physical parameters similar to those observed in the real universe) to determine how objects in the artificial world should move around and interact with one another. Through experience, the mental physics engine essentially learns what sensory stimuli can exist in the world and the physical laws that constrain them, consequently activating networks of all related knowledge to any particular incoming

information. Within such a framework, these arbitrary categories that I taught to participants in the second experiment would simply be considered "unusual" stimuli by the physics engine, which would quickly adapt and eventually activate the necessary networks for processing auditory, tactile, semantic, motor, etc. information. Thus, the supramodal regions discussed earlier would not necessarily be information integrators, but rather they could act either as hubs for moving information or general resource allocators, ensuring that any and all cognitive functions that should engage do engage.

In order to tease apart a more precise role for these seemingly supramodal areas, a new experiment would call for the participants to be placed in the MR scanner before any training and then requiring them to learn the supramodal categories over time (e.g., via trial and error). In this way, the patterns of activity and/or regional connectivity can be monitored before and after the arbitrary supramodal categories acquire a subjective meaning or task-relevance to the participant. With such an experimental design, one could then understand whether information is represented similarly across sensory modalities in the precuneus and posterior insula 1) regardless of the particular task at hand (supporting the idea that these regions are resource allocators) or 2) only after the supramodal stimuli have acquired a specific meaning (supporting the idea that these regions are part of a more specific semantic network, potentially the end result of the cognitive "physics engine").

There are, of course, future directions for more thoroughly investigating the cognitive functions underlying these supramodal cortical areas. For example, if these regions we discovered are information integration regions, then one might expect their activity to change as a function of some confidence or signal strength, such as the neuronal activity often in lateral intraparietal neurons of monkeys (Roitman & Shadlen 2002). The use of methods with superior temporal resolution, such as magnetoencephalography, would allow us to test such an idea.

Additionally, to discriminate whether the regions we found are indeed categorical, we could construct more complex categories with "higher-level" stimuli as members (e.g., arbitrary categories comprising pictures of animals and sounds produced by different musical instruments). This way, we would be able to train participants on different category boundaries within the same experiment (e.g., category A contains brass instruments and wild cats, while category B contains string instruments and reptiles), while maintaining arbitrary semantic relationships within each category, and determine whether the same pattern of effects is present in the same regions. Obtaining similar results after re-training on a different category boundary would lend support to the idea that these regions flexibly represent categorical information (Freedman & Assad 2006). Also, by using more complex stimuli, we could scrutinize whether the observed effects are linked to frequency sweeps or, more generally, temporal information (Battelli et al. 2007). As mentioned in chapter two, it is the case that frequency sweeps have an inherent temporal characteristic to them; thus, one possibility is that all effects discovered are linked to amodal, temporal decision mechanisms. Moreover, despite our results lining up with prior work that employed task-relevant visual stimulation (Fairhall & Caramazza 2013, Wurm & Lingnau 2015), another manner of testing the extent to which the discovered regions are supramodal would be to include visual stimuli in the same experiment as auditory and tactile stimuli. Because we did not directly test visual stimuli alongside the other modalities, there remains the possibility that within association cortex visual information is somehow processed distinctly from information that passed through other sensory cortices. Our current working hypothesis would state that this is not the case.

Newer methods that explore cortical connectivity will also inform our notions regarding these supramodal brain regions. While the functional connectivity results from chapter three do allow us to make some inferences regarding communication within the network, the analysis

itself ultimately returns correlations that tell us no information about directionality (Friston 2011). Instead, thanks to major computational improvements in number crunching, using diffusion information coupled with probabilistic fiber tracking (Basser et al. 1994, Mori & van Zijl 2002) and dynamic causal modeling (Friston et al. 2003)can show us which regions are anatomically connected and also allow us to infer the direction in which information may be flowing between such regions. By treating supramodal regions as seed regions in such a connectivity analysis, one could essentially infer to which other brain regions such supramodal information is projecting. Analyses of this nature can help us to restrict further analyses to specific brain regions and then test hypotheses regarding the extent to which information represented at each of these regions is supramodal. First of all, one analysis could indicate to us the directionality between the precuneus and posterior insula connections, or if the particular regions we discovered connect at all. Secondly, and more significantly, imagine that a fiber tracking analysis reveals that the precuneus projects to a completely different region of cortex. We could then use this data-driven approach to define a new region-of-interest and perform a series of multivariate analyses within the voxels in this newly discovered region rather than relying on searchlight analyses (Kriegeskorte et al. 2006, Oosterhof et al. 2011) and massively losing statistical power: i.e., a *connectivity*-based region-of-interest definition.

Combining such analyses would also allow us to ask more specific questions regarding the relevant information processing. For example, fiber tracking combined with direct causal modeling might allow researchers to follow unisensory regions to multimodal or supramodal regions of cortex and expose potential differences in information representations. Then, by modeling projecting out of supramodal regions, one might discover either another supramodal region or even potentially an 'amodal' region, which would permit us to theorize more specifically about the functionality of supramodal regions: are supramodal regions merely hubs

for forwarding information or do they perform their own processing? Do supramodal regions process unimodal information congruently and output amodal representations? If so, do all supramodal regions share this behavior? What is the format of this information, and can we observe it dynamically changing? These are just a small sample of related questions that new analysis methods and increasingly powerful computing hardware can hope to answer.

## CONCLUSIONS

While the process of categorization has been considered a fundamental function underlying perceptual decision making, the extent to which categorization is a supramodal process remains unknown. With two experiments, this dissertation attempted to reveal more information about the categorization process first by challenging the notion that the frontal lobes play the predominant role in categorization and secondly by exploiting decoding analyses in a new paradigm aimed at uncovering representations of information that are similar across different sensory modalities.

Additionally, we attempted to provide a foundation for the field of perceptual decision making to take a renewed perspective toward the role of the human parietal cortex in perceptual categorization, both in terms of abstractly representing task-relevant information, regardless of sensory modality, and in terms of containing flexible, category-free resources. Furthermore, beyond merely mapping patterns of activity onto the structural architecture of the brain, more crucially from a cognitive science perspective, we demonstrated with pattern classification techniques that supramodal information representations do exist at some level of the functional architecture during perceptual decision making.

By adding this work to the field of cognitive neuroscience, we hope to have pioneered a manner of investigating non-visual information in the human brain, in order to refine theories

pertaining to and start new discussions regarding the cognitive processes that underlie perceptual decisions and the anatomical structures in which they reside.

# REFERENCES


Basser PJ, Mattiello J, LeBihan D. 1994. Estimation of the effective self-diffusion tensor from the NMR spin echo. *Journal of magnetic resonance. Series B* 103: 247-54

Battelli L, Pascual-Leone A, Cavanagh P. 2007. The 'when' pathway of the right parietal lobe. *Trends in cognitive sciences* 11: 204-10

Beauchamp MS, Lee KE, Argall BD, Martin A. 2004. Integration of auditory and visual information about objects in superior temporal sulcus. *Neuron* 41: 809–23

Bennur S, Gold JI. 2011. Distinct representations of a perceptual decision and the associated oculomotor plan in the monkey lateral intraparietal area. *The Journal of neuroscience* 31: 913-21

Binder JR, Desai RH. 2011. The neurobiology of semantic memory. *Trends in cognitive sciences* 15: 527-36

Binder JR, Liebenthal E, Possing ET, Medler DA, Ward BD. 2004. Neural correlates of sensory and decision processes in auditory object identification. *Nature neuroscience* 7: 295-301

Brainard DH. 1997. The Psychophysics Toolbox. *Spatial Vision* 10: 433-36

Britten KH, Newsome WT, Shadlen MN, Celebrini S, Movshon JA. 1996. A relationship between behavioral choice and the visual responses of neurons in macaque MT. *Visual Neuroscience* 13: 87-100

Calvert GA. 2001. Crossmodal Processing in the Human Brain: Insights from Functional Neuroimaging Studies. *Cerebral cortex* 11: 1110–23

Cavanna AE, Trimble MR. 2006. The precuneus: a review of its functional anatomy and behavioural correlates. *Brain* 129: 564-83

Chang CC, Lin CJ. 2011. LIBSVM: A Library for Support Vector Machines. *ACM Transactions on Intelligent Systems and Technology* 2: 1-27

Chang LJ, Yarkoni T, Khaw MW, Sanfey AG. 2013. Decoding the role of the insula in human cognition: functional parcellation and large-scale reverse inference. *Cerebral cortex* 23: 739-49

Cisek P, Kalaska JF. 2005. Neural correlates of reaching decisions in dorsal premotor cortex: specification of multiple direction choices and final selection of action. *Neuron* 45: 801-14

Cisek P, Kalaska JF. 2010. Neural mechanisms for interacting with a world full of action choices. *Annual review of neuroscience* 33: 269-98

Cloutman LL, Binney RJ, Drakesmith M, Parker GJ, Lambon Ralph MA. 2012. The variation of function across the human insula mirrors its patterns of structural connectivity: evidence from in vivo probabilistic tractography. *NeuroImage* 59: 3514-21

Deco G, Rolls ET, Albantakis L, Romo R. 2013. Brain mechanisms for perceptual and reward-related decision-making. *Progress in Neurobiology* 103: 194-213.

De Benedictis A, Duffau H, Paradiso B, Grandi E, Balbi S, et al. 2014. Anatomo-functional study of the temporo-parieto-occipital region: dissection, tractographic and brain mapping evidence from a neurosurgical perspective. *Journal of anatomy* 225: 132-51

De Lucia M, Tzovara A, Bernasconi F, Spierer L, Murray MM. 2012. Auditory perceptual decision-making based on semantic categorization of environmental sounds. *NeuroImage* 60: 1704-15

Deprez S, Vandenbulcke M, Peeters R, Emsell L, Amant F, Sunaert S. 2013. The functional neuroanatomy of multitasking: combining dual tasking with a short term memory task. *Neuropsychologia* 51: 2251-60

Duffau H, Gatignol P, Mandonnet E, Peruzzi P, Tzourio-Mazoyer N, Capelle L. 2005. New insights into the anatomo-functional connectivity of the semantic system: a study using cortico-subcortical electrostimulations. *Brain* 128: 797-810

Duncan J. 2010. The multiple-demand (MD) system of the primate brain: mental programs for intelligent behaviour. *Trends in cognitive sciences* 14: 172-9

Eger E, Sterzer P, Russ MO, Giraud A, Kleinschmidt A. 2003. Supramodal number representation in human intraparietal cortex. *Neuron* 37: 719–25

Fairhall SL, Caramazza A. 2013. Brain regions that represent amodal conceptual knowledge. *The Journal of neuroscience* 33: 10552-8

Fedorenko E, Duncan J, Kanwisher N. 2013. Broad domain generality in focal regions of frontal and parietal cortex. *Proceedings of the National Academy of Sciences of the United States of America* 110: 16616–21

Filimon F, Philiastides MG, Nelson JD, Kloosterman NA, Heekeren HR. 2013. How embodied is perceptual decision making? Evidence for separate processing of perceptual and motor decisions. *The Journal of neuroscience* 33: 2121-36

Fischl B, Sereno MI, Tootell RBH, Dale AM. 1999. High-Resolution Intersubject Averaging and a Coordinate System for the Cortical Surface. *Human brain mapping* 8: 272-84

Fitzgerald JK, Freedman DJ, Assad JA. 2011. Generalized associative representations in parietal cortex. *Nature neuroscience* 14: 1075-9

Freedman DJ, Assad JA. 2006. Experience-dependent representation of visual categories in parietal cortex. *Nature* 443: 85-8

Freedman DJ, Assad JA. 2011. A proposed common neural mechanism for categorization and perceptual decisions. *Nature neuroscience* 14: 143-6

Friston KJ. 2011. Functional and effective connectivity: a review. *Brain connectivity* 1: 13-36

Friston KJ, Harrison L, Penny W. 2003. Dynamic causal modelling. *NeuroImage* 19: 1273-1302

Friston KJ, Worsley KJ, Frackowiak RSJ, Mazziotta JC, Evans AC. 1994. Assessing the significance of focal activations using their spatial extent. *Human brain mapping* 1: 210-20

Gallese V, Lakoff G. 2005. The Brain's concepts: the role of the Sensory-motor system in conceptual knowledge. *Cognitive neuropsychology* 22: 455-79

García-Pérez MA. 2000. Optimal setups for forced-choice staircases with fixed step sizes. *Spatial Vision* 13: 431-48

Goebel R, Esposito F, Formisano E. 2006. Analysis of functional image analysis contest (FIAC) data with brainvoyager QX: From single-subject to cortically aligned group general linear model analysis and self-organizing group independent component analysis. *Human brain mapping* 27: 392-401

Goebel R, van Atteveldt N. 2009. Multisensory functional magnetic resonance imaging: a future perspective. *Experimental brain research* 198: 153-64

Gold JI, Shadlen MN. 2000. Representation of a perceptual decision in developing oculomotor commands. *Nature* 404: 390-94

Gold JI, Shadlen MN. 2001. Neural computations that underlie decisions about sensory stimuli. *Trends in cognitive sciences* 5: 10-16

Gold JI, Shadlen MN. 2007. The neural basis of decision making. *Annual review of neuroscience* 30: 535-74

Grinband J, Hirsch J, Ferrera VP. 2006. A neural representation of categorization uncertainty in the human brain. *Neuron* 49: 757-63

Hadjikhani N, Roland PE. 1998. Cross-modal transfer of information between the tactile and the visual representations in the human brain: A positron emission tomographic study. *The Journal of neuroscience* 18: 1072-84

Haxby JV, Gobbini MI, Furey ML, Ishai A, Schouten JL, Pietrini P. 2001. Distributed and overlapping representations of faces and objects in ventral temporal cortex. *Science* 293: 2425-30

Hayasaka S, Nichols TE. 2003. Validating cluster size inference, random field and permutation methods. *NeuroImage* 20: 2343-56

Hebart MN, Donner TH, Haynes JD. 2012. Human visual and parietal cortex encode visual choices independent of motor plans. *NeuroImage* 63: 1393-403

Heekeren HR, Marrett S, Bandettini P, Ungerleider LG. 2004. A general mechanism for perceptual decision-making in the human brain. *Nature* 431: 859-62

Heekeren HR, Marrett S, Ruff DA, Bandettini PA, Ungerleider LG. 2006. Involvement of human left dorsolateral prefrontal cortex in perceptual decision making is independent of response modality. *Proceedings of the National Academy of Sciences of the United States of America* 103: 10023-8

Heekeren HR, Marrett S, Ungerleider LG. 2008. The neural systems that mediate human perceptual decision making. *Nature reviews. Neuroscience* 9: 467-79

Hernandez A, Zainos A, Romo R. 2002. Temporal evolution of a decision-making process in medial premotor cortex. *Neuron* 33: 959-72

Ho TC, Brown S, Serences JT. 2009. Domain general mechanisms of perceptual decision making in human cortex. *The Journal of neuroscience* 29: 8675-87

Holloway ID, Price GR, Ansari D. 2010. Common and segregated neural pathways for the processing of symbolic and nonsymbolic numerical magnitude: an fMRI study. *NeuroImage* 49: 1006-17

Hsieh IH, Fillmore P, Rong F, Hickok G, Saberi K. 2012. FM-selective Networks in Human Auditory Cortex Revealed Using fMRI and Multivariate Pattern Classification. *Journal of cognitive neuroscience* 24: 1896-907

Hubbard EM, Ramachandran VS. 2005. Neurocognitive mechanisms of synesthesia. *Neuron* 48: 509-20

Ivanoff J, Branning P, Marois R. 2009. Mapping the pathways of information processing from sensation to action in four distinct sensorimotor tasks. *Human brain mapping* 30: 4167-86

Kaiser J, Lennert T, Lutzenberger W. 2007. Dynamics of oscillatory activity during auditory decision making. *Cerebral cortex* 17: 2258-67

Klemen J, Chambers CD. 2012. Current perspectives and methods in studying neural mechanisms of multisensory interactions. *Neuroscience and biobehavioral reviews* 36: 111-33

Koechlin E, Ody C, Kouneiher F. 2003. The architecture of cognitive control in the human prefrontal cortex. *Science* 302: 1181-5

Kriegeskorte N, Goebel R, Bandettini P. 2006. Information-based functional brain mapping. *Proceedings of the National Academy of Sciences of the United States of America* 103: 3863-8

Langner R, Kellermann T, Eickhoff SB, Boers F, Chatterjee A, et al. 2012. Staying responsive to the world: modality-specific and -nonspecific contributions to speeded auditory, tactile, and visual stimulus detection. *Human brain mapping* 33: 398-418

Laurienti PJ, Wallace MT, Maldjian JA, Susi CM, Stein BE, Burdette JH. 2003. Cross-modal sensory processing in the anterior cingulate and medial prefrontal cortices. *Human brain mapping* 19: 213-23

Leaver AM, Rauschecker JP. 2010. Cortical representation of natural complex sounds: effects of acoustic features and auditory object category. *The Journal of neuroscience* 30: 7604-12

Lee YS, Turkeltaub P, Granger R, Raizada RD. 2012. Categorical speech processing in Broca's area: an fMRI study using multivariate pattern-based analysis. *The Journal of neuroscience* 32: 3942-8

Lemus L, Hernandez A, Luna R, Zainos A, Romo R. 2010. Do sensory cortices process more than one sensory modality during perceptual judgments? *Neuron* 67: 335-48

Lemus L, Hernandez A, Romo R. 2009. Neural codes for perceptual discrimination of acoustic flutter in the primate auditory cortex. *Proceedings of the National Academy of Sciences of the United States of America* 106: 9471–76

Levine SM and Schwarzbach J. Under review. Parietal representations allow auditory and tactile perceptual decisions.

Lingnau A, Downing PE. 2015. The lateral occipitotemporal cortex in action. *Trends in cognitive sciences* 19: 268-77

Margulies DS, Vincent JL, Kelly C, Lohmann G, Uddin LQ, et al. 2009. Precuneus shares intrinsic functional architecture in humans and monkeys. *Proceedings of the National Academy of Sciences of the United States of America* 106: 20069-74

McKee JL, Riesenhuber M, Miller EK, Freedman DJ. 2014. Task dependence of visual and category representations in prefrontal and inferior temporal cortices. *The Journal of neuroscience* 34: 16065-75

Mori S, van Zijl PC. 2002. Fiber tracking: principles and strategies - a technical review. *NMR in biomedicine* 15: 468-80

Myers EB, Blumstein SE, Walsh E, Eliassen J. 2009. Inferior frontal regions underlie the perception of phonetic category invariance. *Psychological science* 20: 895-903

Naghavi HR, Eriksson J, Larsson A, Nyberg L. 2007. The claustrum/insula region integrates conceptually related sounds and pictures. *Neuroscience letters* 422: 77-80

Newsome WT, Britten KH, Movshon JA. 1989. Neuronal correlates of a perceptual decision. *Nature* 341: 52-54

Noppeney U, Ostwald D, Werner S. 2010. Perceptual decisions formed by accumulation of audiovisual evidence in prefrontal cortex. *The Journal of neuroscience* 30: 7434-46

O'Connell RG, Dockree PM, Kelly SP. 2012. A supramodal accumulation-to-bound signal that determines perceptual decisions in humans. *Nature neuroscience* 15: 1729-35

Oosterhof NN, Wiestler T, Downing PE, Diedrichsen J. 2011. A comparison of volume-based and surface-based multi-voxel pattern analysis. *NeuroImage* 56: 593-600

Penny W, Friston K. 2003. Mixtures of general linear models for functional neuroimaging. *IEEE Transactions on Medical Imaging* 22: 504-14

Philiastides MG, Auksztulewicz R, Heekeren HR, Blankenburg F. 2011. Causal role of dorsolateral prefrontal cortex in human perceptual decision making. *Current biology* 21: 980-3

Pleger B, Ruff CC, Blankenburg F, Bestmann S, Wiech K, et al. 2006. Neural coding of tactile decisions in the human prefrontal cortex. *The Journal of neuroscience* 26: 12596-601

Ploran EJ, Nelson SM, Velanova K, Donaldson DI, Petersen SE, Wheeler ME. 2007. Evidence accumulation and the moment of recognition: dissociating perceptual recognition processes using fMRI. *The Journal of neuroscience* 27: 11912-24

Preuschhof C, Heekeren HR, Taskin B, Schubert T, Villringer A. 2006. Neural correlates of vibrotactile working memory in the human brain. *The Journal of neuroscience* 26: 13231-9

Rishel CA, Huang G, Freedman DJ. 2013. Independent category and spatial encoding in parietal cortex. *Neuron* 77: 969-79

Robinson S, Jovicich J. 2011. B0 mapping with multi-channel RF coils at high field. *Magnetic resonance in medicine* 66: 976-88

Roitman JD, Shadlen MN. 2002. Response of neurons in the lateral intraparietal area during a combined visual discrimination reaction time task. *The Journal of neuroscience* 22: 9475-89

Romo R, Hernandez A, Zainos A. 2004. Neuronal Correlates of a Perceptual Decision in Ventral Premotor Cortex. *Neuron* 41: 165-73

Romo R, Hernandez A, Zainos A, Lemus L, Brody CD. 2002. Neuronal correlates of decision-making in secondary somatosensory cortex. *Nature neuroscience* 11: 1217-25

Roskies AL, Fiez JA, Balota DA, Raichle ME, Petersen SE. 2001. Task-dependent modulation of regions in the left inferior frontal cortex during semantic processing. *Journal of cognitive neuroscience* 13: 829-43

Salinas E, Hernandez A, Zainos A, Romo R. 2000. Periodicity and Firing Rate As Candidate Neural Codes for the Frequency of Vibrotactile Stimuli. The *Journal of neuroscience* 20: 5503-15

Schwarzbach J. 2011. A simple framework (ASF) for behavioral and neuroimaging experiments based on the psychophysics toolbox for MATLAB. *Behavior research methods* 43: 1194-201

Shadlen MN, Britten KH, Newsome WT, Movshon JA. 1996. A Computational Analysis of the Relationship between Neuronal and Behavioral Responses to Visual Motion. The *Journal of neuroscience* 16: 1486-510

Shadlen MN, Kiani R, Hanks TD, Churchland AK. 2008. Neurobiology of decision making: An intentional framework In *Better Than Conscious? Decision Making, the Human Mind, and Implications For Institutions*, ed. C Engel, W Singer, pp. 71-101. Cambridge: MIT Press

Shadlen MN, Newsome WT. 1996. Motion perception: Seeing and deciding. *Proceedings of the National Academy of Sciences of the United States of America* 93: 628-33

Shadlen MN, Newsome WT. 2001. Neural Basis of a Perceptual Decision in the Parietal Cortex (Area LIP) of the Rhesus Monkey. *Journal of neurophysiology* 86: 1916-36

Shomstein S, Yantis S. 2004. Control of attention shifts between vision and audition in human cortex. *The Journal of neuroscience* 24: 10702-6

Simanova I, Hagoort P, Oostenveld R, van Gerven MA. 2014. Modality-independent decoding of semantic information from the human brain. *Cerebral cortex* 24: 426-34

Siok WT, Jin Z, Fletcher P, Tan LH. 2003. Distinct brain regions associated with syllable and phoneme. *Human brain mapping* 18: 201-07

Smith SM, Nichols TE. 2009. Threshold-free cluster enhancement: addressing problems of smoothing, threshold dependence and localisation in cluster inference. *NeuroImage* 44: 83-98

Spunt RP, Lieberman MD. 2012. Dissociating modality-specific and supramodal neural systems for action understanding. *The Journal of neuroscience* 32: 3575-83

Staeren N, Renvall H, De Martino F, Goebel R, Formisano E. 2009. Sound categories are represented as distributed patterns in the human auditory cortex. *Current biology* 19: 498-502

Swaminathan SK, Freedman DJ. 2012. Preferential encoding of visual categories in parietal cortex compared with prefrontal cortex. *Nature neuroscience* 15: 315-20

Swaminathan SK, Masse NY, Freedman DJ. 2013. A comparison of lateral and medial intraparietal areas during a visual categorization task. *The Journal of neuroscience* 33: 13157-70

Tal N, Amedi A. 2009. Multisensory visual-tactile object related network in humans: insights gained using a novel crossmodal adaptation approach. *Experimental brain research* 198: 165-82

Talairach J, Tournoux P. 1988. *Co-planar stereotaxic atlas of the human brain. 3-Dimensional proportional system: an approach to cerebral imaging*. Thieme.

Tamber-Rosenau BJ, Dux PE, Tombu MN, Asplund CL, Marois R. 2013. Amodal processing in human prefrontal cortex. *The Journal of neuroscience* 33: 11573-87

Tenenbaum J. 21 April 2015. Reverse-engineering common sense: Modeling human intelligence with probabilistic programs and program induction. Federation of European Neuroscience Societies. Copenhagen, Denmark. Keynote Address.

Thompson-Schill SL, D'Esposito M, Aguirre GK, Farah MJ. 1997. Role of left inferior prefrontal cortex in retrieval of semantic knowledge: A reevaluation. *Proceedings of the National Academy of Sciences of the United States of America* 94: 14792-97

van Atteveldt N, Formisano E, Goebel R, Blomert L. 2004. Integration of letters and speech sounds in the human brain. *Neuron* 43: 271-82

van Atteveldt NM, Blau VC, Blomert L, Goebel R. 2010. fMR-adaptation indicates selectivity to audiovisual content congruency in distributed clusters in human superior temporal cortex. *BMC neuroscience* 11: 11

van Kemenade BM, Seymour K, Wacker E, Spitzer B, Blankenburg F, Sterzer P. 2014. Tactile and visual motion direction processing in hMT+/V5. *NeuroImage* 84: 420-7

Wang XJ. 2002. Probabilistic decision making by slow reverberation in cortical circuits. *Neuron* 36: 955–68.

Wong KF, Wang XJ. 2006. A recurrent network mechanism of time integration in perceptual decisions. *The Journal of neuroscience* 26: 1314–28.

Woo CW, Krishnan A, Wager TD. 2014. Cluster-extent based thresholding in fMRI analyses: pitfalls and recommendations. *NeuroImage* 91: 412-9

Woolgar A, Hampshire A, Thompson R, Duncan J. 2011. Adaptive coding of task-relevant information in human frontoparietal cortex. *The Journal of neuroscience* 31: 14592-9

Wurm MF, Lingnau A. 2015. Decoding actions at different levels of abstraction. *The Journal of neuroscience* 35: 7727-35

Yantis S, Schwarzbach J, Serences JT, Carlson RL, Steinmetz MA, et al. 2002. Transient neural activity in human parietal cortex during spatial attention shifts. *Nature neuroscience* 5: 995-1002

Yeo BT, Krienen FM, Sepulcre J, Sabuncu MR, Lashkari D, et al. 2011. The organization of the human cerebral cortex estimated by intrinsic functional connectivity. *Journal of neurophysiology* 106: 1125-65

Zaitsev M, Hennig J, Speck O. 2004. Point spread function mapping with parallel imaging techniques and high acceleration factors: fast, robust, and flexible method for echo-planar imaging distortion correction. *Magnetic resonance in medicine* 52: 1156-66

Zhang S, Li CS. 2012. Functional connectivity mapping of the human precuneus by resting state fMRI. *NeuroImage* 59: 3548-62